Det Kgl. Danske Videnskabernes Selskab
Mathematisk-fysiske Meddelelser. I, 11.

ON THE LICHTENBERG FIGURES

PART I. A PRELIMINARY INVESTIGATION

BY

P. O. PEDERSEN

KØBENHAVN
HOVEDKOMMISSIONÆR: ANDR. FRED. HØST & SØN, KGL. HOF-BOGHANDEL
BIANCO LUNOS BOGTRYKKERI
1919

Chapter I.

Introduction and Historical Remarks.

THE LICHTENBERG dust figures can be made in many ways; one of the simplest is as follows: An electrically neutral plate P of ebonite (Fig. 1) is placed on a metal disk B. From the knob K of a Leyden jar L a spark is passed to the

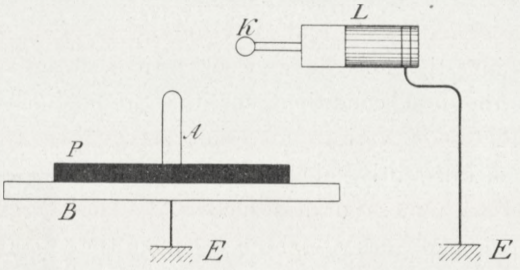

Fig. 1. Simple Lichtenberg Arrangement.

small metal rod A placed on P. The rod A is then removed and the plate P powdered with lycopodium, flour sulphur, or some other suitable powder. Mixtures of different powders may also be used with advantage. The dust settled on P then forms a LICHTENBERG figure. If K has been positive the shape of the figure is as shown in Fig. 2, while Fig. 3 shows the result for K negative.

LICHTENBERG[1, 2] observed these figures for the first time in the year 1777*; since then they have formed the subject of a long series of investigations. And naturally so: the figures are beautiful and the difference between the positive and negative ones very striking. It may therefore be expected that a

* For references see the bibliography at the end of the paper.

closer study of this phenomenon would give valuable information on the nature of electricity, and the history of these figures is also very closely connected with the history of the theories of electricity — one fluid and two fluid theories —. At present the corresponding literature is mainly of historical interest and we shall therefore only call attention to the papers of P. F. Riess, E. Reitlinger, A. v. Waltenhofen, W. v. Bezold, W. G. Armstrong, A. Oberbeck, and W. Holtz.

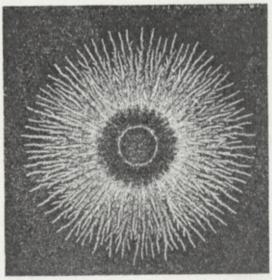

Fig. 2. Positive Lichtenberg Dust Figure. (Air; $p = 760$; $m = 0.8$*)

Many investigations have been carried out in order to ascertain the best conditions for the production of these figures. Plates of various materials have been tried and mixtures of differently coloured powders have been used with more or less success.** The photographic plate has also been used for the recording of transient electrical discharges by J. Brown (1888),[1] E. T. Trouvelot (1888),[1] K. Hansen (1916),[1] and others. These authors have, however, used such high voltages that rather complicated figures, like those in Figs. 4 and 5, have been obtained. Just recently M. Toepler (1917)[1] has published some beautiful photographs of »sliding« electrical discharges (Gleitfunken). All these figures are, however, so complicated that they do not invite a closer study of their features.

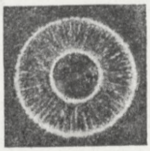

Fig. 3. Negative Dust Figure. (Air; $p = 760$; $m = 0.8$).

* In the following p denotes the gas pressure in millimetres of mercury, l the spark length in millimeters (see Fig. 10), D the diameter of the electrode A, d_0 thickness of insulating plate both in millimeters. m stands for magnification.

** v. Villarsy proposed 1788 the use of a mixture of red lead and flour sulphur. A mixture of 3 powders, viz Carnine, lycopodium, and sulphur has been used by K. Bürker[1].

W. G. Armstrong in 1897 published some simple photographic Lichtenberg figures. Especially some of his positive figures are remarkably pure and simple and many of his plates show very interesting features. The beautiful illustrations — partly in colours — of dust figures, which W. G. Armstrong and H. Stroud[1] published in 1899 also give much valuable information about the Lichtenberg figures.*

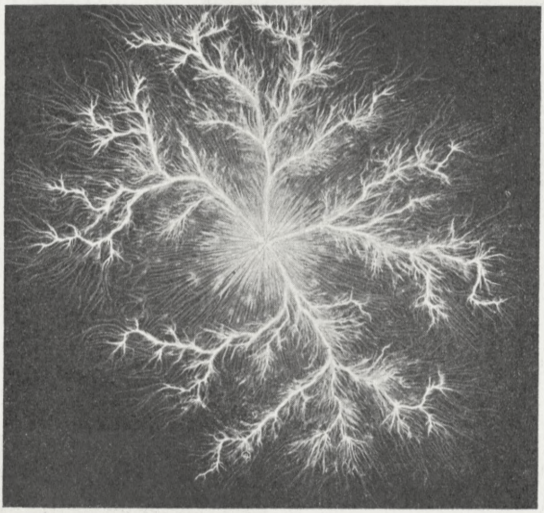

Fig. 4. Positive Discharge with High Voltage.
(Air; $p = 760$; $l = 7$; $D = 0$; $d_0 = 1.4$; $m = 0.7$).

S. Mikola (1917) recently published some beautiful photographs of simple Lichtenberg figures — positive and negative — obtained direct on photographic plates. These figures are very regular and characteristical and exhibit very fine details. The photographical method of Mikola has been used almost exclusively throughout this investigation and this method is also — contrary to Mikola's own observation — applicable to Lichtenberg figures in hydrogen,

* This work of Lord Armstrong seems to be but little known; S. Mikola f. inst. does not mention it.

oxygen, and carbon dioxide, but the figures obtained in these gases are rather faint, especially at lower pressures.

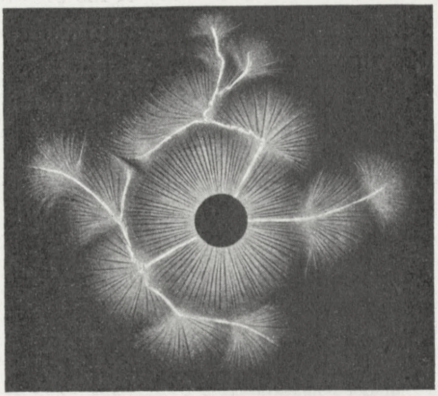

Fig. 5. Negative Discharge with High Voltage. (Air; $p = 760$: $l = 7$; $D = .10$; $d_0 = 1.4$; $m = 0.7$).

Examples of such figures in air are shown in Figs. 6 and 7. In nitrogen and argon the figures are still brighter than in air. In cases where the photographic method gives too faint figures, the ordinary dust method may be used with advantage even if it does not give such delicate details as the photographic one.

Many investigations have formerly been carried out in the hope of getting an explanation of the origination of these figures and of the very remarkable difference between the positive and negative ones. On the whole very little progress has, however, been made. With regard to the former experiments and speculations it is sufficient to refer to the papers mentioned on page 4, which contain ample information on this question.

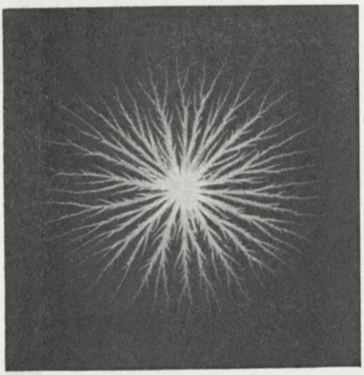

Fig. 6. Normal Positive Figure. (Air; $p=760$; $l=3$; $D=0$; $d_0=1.4$; $m=1$).

E. Reitlinger[1, 2], in 1860-61, tried to explain the figures on the hypothesis that electrical particles during the discharge travel from the electrode outwards through the

surrounding gas. The positive and negative particles move in different manners, this being the cause for the difference between the positive and negative figures. Even if REITLINGER was — and necessarily must have been — unable to give a satisfactory explanation of the phenomenon, his ideas were remarkably sound and his proofs of the close connection between these figures and the electrical properties of the gas seem conclusive. He had, in fact, solved this intricate question as far as it could be solved at that time. His views were, however, in the main only supported by A. v. WALTENHOFEN[1], and later investigators have worked along other lines. As late as 1905 W. HOLTZ[1] even comes to the conclusion that the nature of the gas, nay even gas altogether, is of little importance with regard to the LICHTENBERG figures.

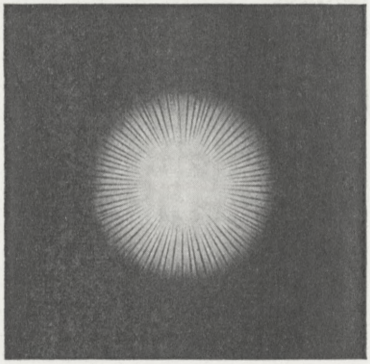

Fig. 7. Normal Negative Figure. (Air; $p=760$; $l=7$; $D=0$; $d_0=1.4$; $m=1$).

According to W. v. BEZOLD[1, 2, 3, 4], who had carried out a series of important investigations on this subject, the figures are due to air currents. He supposes — rather arbitrarily — that the negative figure is formed by air currents going outwards from the electrode while air currents in the opposite direction produce the positive ones. He tried to prove this hypothesis by experiments on powdered water. By means of a tube, the end of which was just at the surface of the powdered water, a small amount could suddenly be either added to or drawn away from the bulk of water. In the first case a »negative« and in the last a »positive« figure appeared. The resemblance is, however, not very striking. As a conclusive proof he considered the following circumstance: He found,

that the exterior part of the figure formed from a positive, ring-shaped electrode had the normal positive appearance, but the interior part was of negative character, and similarly for negative discharges. E. Mach and S. Doubrava[1] denied the correctness hereof, and Figs. 8 and 9 show that these authors were right: the exterior and the interior part of the figures are either both of positive or both of negative character. The mistake made by v. Bezold is, however, very excusable; it would be almost impossible to settle this question by the dust method. We shall later see that the Lichtenberg figures are formed with such great velocity that air currents cannot have any appreciable influence.

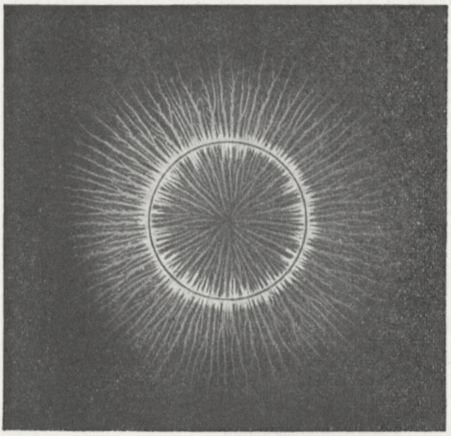

Fig. 8. Positive Figure obtained with Ring-shaped Electrode. (Air; $p = 760$; $l = 3$; $m = 0.9$).

G. Quincke[1] sees in the often mentioned figures an interaction of different sorts of rays: positive rays able to penetrate millimetres of insulators, negative rays, and retrograde rays of two different kinds. His positive and negative rays even seem to be of composite nature — consisting of both quickly moving particles and electromagnetic radiation. This explanation of the Lichtenberg figures will hardly be accepted as satisfactory.

S. Mikóla[1] in his above mentioned paper also gives some new and rather startling hypotheses. His views may be summarized as follows: Electromagnetic impulses are emitted from the edge of the condenser, when impulsively discharged. These impulses, travelling along the conductor, produce po-

sitive and negative ions of great velocity, which move rapidly along the conductor and with certain intervals of time cause the emission of electromagnetic impulses, which in turn liberate ions from the conductor. Even accepting all these rather strange hypotheses it is not easy to see how they can afford a satisfactory explanation of the great differences between the positive and negative figures.

Notwithstanding the great amount of work which has been spent in order to elucidate this question, we know, up to the present, little more about the origination of these figures than LICHTENBERG did. This fact will probably explain the present lack of interest in this question. Neither in J. J. THOMSON: Conduction of Electricity through Gases (1906), nor in J. S. TOWNSEND: Electricity in Gases (1915), nor in A. WINKELMANN: Handbuch der Physik (1908), is the name of LICHTENBERG to be found.

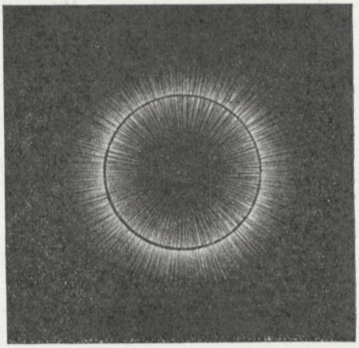

Fig. 9. Negative Figure obtained with Ringshaped Electrode. (Air; $p = 760$; $l = 6$; $m = 0.9$).

The aim of the present investigation is to throw some light on the main features of the origination of the LICHTENBERG figures. The results obtained seem to indicate that the elucidation of the origination of these figures will probably prove to be of great importance for the study of the process of ionization of gases and for the molecular and atomic dynamics.

The present paper deals only with a preliminary investigation of the general features of the LICHTENBERG figures and the numerical results are to be considered as provisional. Several more detailed investigations connected with this problem are being carried out at present.

Chapter II.

General Remarks on the Origination of the Lichtenberg Figures.

1. Most of the experiments described in the following are carried out with the arrangement shown in Fig. 10. The condenser C can be charged through the great resistances R_1

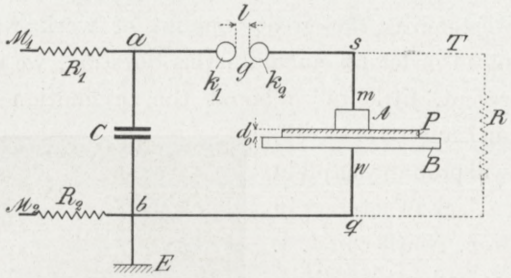

Fig. 10. Diagram of Circuit for ordinary Lichtenberg Figures.

and R_2 from a small influence machine connected to M_1 and M_2. The resistance R_1 is a slate pencil, and R_2 either a slate pencil or a thin piece of wood. The spark gap g has 4 cm. brass balls, k_1 and k_2. The small electrode A generally rests on the sensitive film of the dry plate P placed on the metal disk B which is connected through the wire nqb and resistance R_2 with one pole of the electric machine. The connecting wire is earthed at b. Electrode A, plate P, and electrode B form what we will call the Lichtenberg gap (L. G.). When working with other gases than air and in rarefied gases the L. G. was enclosed in a bell jar, the wire m being carried air-tight through the side of the jar. The figures are said to be positive when k_1 is positive before the spark passes over. The electrical machine must be rotated very slowly, especially when working with short spark lengths, in order to get a definite sparking voltage and to avoid the passage of more than one spark each time.

The L. G. was generally shunted by a slate pencil R or some other great resistance. This shunt increases the damping of the oscillations in the circuit $CgAPBC$, but its main object is to bring about that the potential of the electrode A before and after a discharge is equal to that of the earth connection E. Otherwise the removal af A may cause a new discharge, and other complications may arise.

Different dry plates have been tried; the most satisfactory results have been obtained with Hauff's Roentgen plates.

The figures only appear if the P. D. across the L. G. is altered in an impulsive or sudden manner and not if the potential of A is raised gradually — the spark gap g being short circuited and the shunt R removed. This observation was made by T. P. Reiss (1864)[1]; S. Mikola[1] herefrom draws the conclusion that the formation of these figures is due to the rapid variation in the potential across the L. G., and does not take place because and when the P. D. has reached a certain value. He considers that this form of discharge is produced when the innermost ends of the lines of force travelling along the electrode A are suddenly stopped; the sharp bends thereby produced on these lines then travel out along them with the velocity of light, and constitute an electromagnetic radiation of the same kind as Roentgen rays.

It is, however, not necessary to introduce new and rather doubtful hypotheses in order to explain the necessity of a very steep rise in the P. D. across the L. G. in order to obtain Lichtenberg figures. We need only consider the circumstances connected with the commencement of a Lichtenberg discharge a little closer. The spark in g (see Fig. 10) starts an electric wave along the wire k_2m. The maximum voltage of this wave is partially reflected at A and the reflected wave travels back along mk_2. The potential at A is the sum of the potential of the incident and of the reflected wave, and if the capacity of A is small, the maximum potential

at A will be almost equal to twice the sparking voltage. In comparing the effect of a stationary voltage across the L. G. with that of an impulsive voltage caused by a spark as in Fig. 10, the former must be about twice the sparking voltage. But a statical voltage however great does not produce Lichtenberg figures. So far Mikola is right. A static voltage in this connection means a voltage which has been raised very slowly. At a certain stage of this charging of the electrode A the intensity of the electric field between A and the plate P reaches a value at which ionization by collision commences. But no disruptive discharge takes place because the ionization current is charging the surface of the insulating plate P and thus automatically keeping the intensity of the electric field between A and P below a certain value, a value too low to produce sparking. Simultaneously with the process of charging of P a diffusion of this charge along the surface of the plate is going on, but the electric field nowhere attains a value sufficiently high to produce disruptive discharges of any kind. It is not before the diffused charge in sufficient quantity has reached the edge of the plate that the electric field there becomes sufficiently intense to produce a spark, which increases in length until it connects A and B. Photographs of such sliding sparks are reproduced in Armstrong's work, and these sparks have been very carefully investigated by Toepler.

The reason why the Lichtenberg figures do not appear with slowly varying potentials is simply that the intensity af the electric field in this case does not attain the necessary high value. With a rapidly varying potential there is, however, a possibility of obtaining sufficiently strong fields because it takes some time to establish the compensating charge on the plate P.

At the edge of the coatings of leyden jars and similar condensers analogous conditions are to be found. If the po-

tential varies slowly, the ionization which takes place at the edge causes the electric charges to be distributed in such a way that the electric field nowhere attains a value high enough to produce strong ionization, and a quasi-stationary state is established, during which a feeble current leaks from one electrode to the other. If the potential changes very rapidly there is not sufficient time for effecting this distribution of the charge, and the field may attain such high values that a figure appears. If the condenser is subjected to high frequency voltages, such LICHTENBERG discharges appear twice every period, and the heat caused hereby will often crack the glass.

As pointed out it is necessary to apply rapidly varying potentials in order to get the necessary intensity of the electric field. On the other hand the P. D. across the L. G. must not be kept too long or with too high a value after the LICHTENBERG discharge has been started. Otherwise, in addition to the first formed, regular LICHTENBERG figure, there will appear other more complicated ones and, if the P. D. is kept on for say about 1.10^{-6} second, a spark generally occurs. In order to obtain pure and simple LICHTENBERG figures the L. G. must be subjected to a very high impulsive voltage of very short duration. And to this very impulsivity the LICHTENBERG figures owe the great importance they undoubtedly have for the study of discharges in gases. They show the effect of a very strong field of extremely short duration. The field may be so strong that it cannot be sustained for say 10^{-6} second without resulting in a disruptive discharge in which most of the effects of the initial or LICHTENBERG state of the discharge would be altogether lost. It seems difficult to imagine any other method by which this initial state of ionization could be investigated — and so easily and conveniently investigated — the LICHTENBERG figures affording an almost instantaneous picture of what is going on during this initial ionization.

The duration of a Lichtenberg discharge is about 1.10^{-8} second as will be shown later on. W. v. Bezold and others working with dust figures state that the origination of these figures takes a comparatively long time. They have probably been led to this mistake by the relatively slow movements which are to be seen in the dust even several minutes after the formation of the figures. These movements are due to electrostatic forces on the dust particles and have nothing to do with the origination of the Lichtenberg figures.

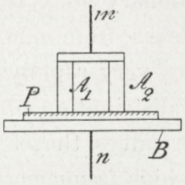

Fig. 11. Lichtenberg Figures from several Parallel Electrodes.

The Lichtenberg figures originate and develop with great regularity and exactness. This is easily shown by placing

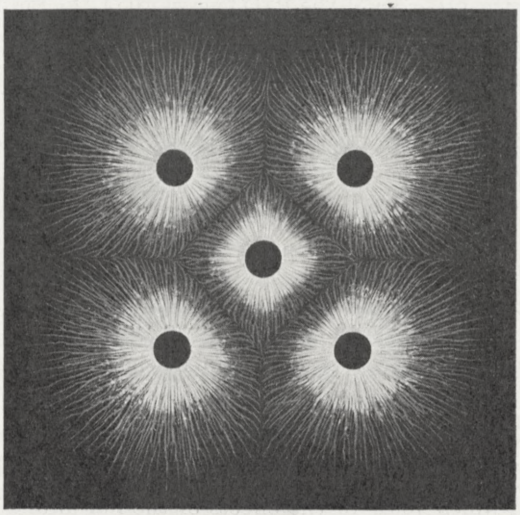

Fig- 12. Positive Figure from five Electrodes. (Air; $p = 760$; $l = 6$; $d_0 = 1.3$; $m = 0.8$).

several electrodes connected in parallel on the same plate as indicated in Fig. 11, where the electrodes A_1 and A_2 are connected to a metal plate and rest on the photographic

plate *P*. Separate LICHTENBERG figures then start simultaneously from the different electrodes, and the boundary lines between the different figures are very regular, showing the great precision with which the figures originate. Fig. 12 shows a positive and Fig. 13 a negative figure of this kind.

W. v. BEZOLD and S. MIKOLA have proved that the shape and the size of the figures are independent of the nature of the electrode, provided only it is a good conductor. This may be easily confirmed by the fact that the electrodes in the Figures 12 and 13 may be made of different metals without thereby in any way altering the shape and size of the combined figure. If on the other hand a very bad conductor is used as electrode, the appearance of the figures is altered as pointed out by W. v. BEZOLD and S. P. THOMPSON[1]. These irregular figures have not been included in our investigation.

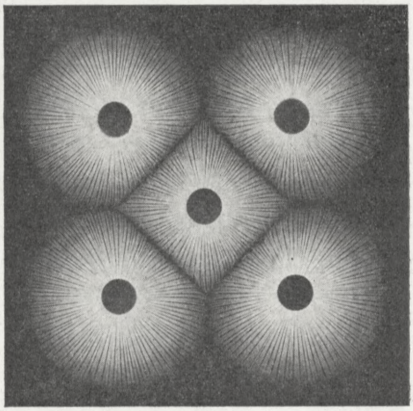

Fig. 13. Negative Figure from five Electrodes. (Air; $p = 760$; $l = 6$; $d_0 = 1.3$; $m = 0.8$).

Even if the metal electrode is put in a shoe of insulating material, for instance ebonite, say 1 millimetre thick, a regular LICHTENBERG figure may be formed. The effect of the shoe is a reduction in size of the figure and some retardation in the discharge. In Fig. 14 and Fig. 15 the right electrode is with, the left one without, shoe and both electrodes are connected to the same metal plate (see Fig. 11).

A similar effect is produced by placing a plate of insulating material across the path of the figure as shown in Fig. 16. A

glass plate 0.77 mm. thick was cemented to the sensitive film by means of picein. It is seen that the figure is not cut off by the vertical glass plate but its range is somewhat reduced.

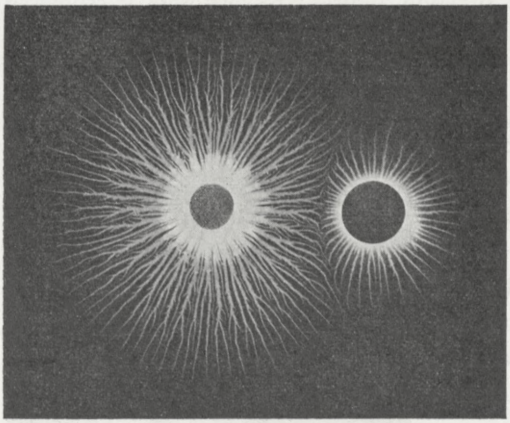

Fig. 14. Positive Figure from two Parallel Brass Electrodes, the Right one with a Shoe of Ebonite, 1 mm. thick. (Air; $p = 760$; $l = 8$; $d_0 = 1.4$; $m = 1$).

G. Quincke explains this behaviour of the Lichtenberg figures by postulating that these figures are due to some specific kind of rays which are able to pass through insulators. A closer study of Fig. 16 does not lend support to Quincke's view: the »rays« outside the plate are not extensions of the inside »rays«, but start from the outer surface of the glass plate and in a direction very nearly normal to this plate. The outside part of the figure is no doubt due to the electric field just outside the glass plate caused by the sudden accumulation of charge on the inner side of this plate.

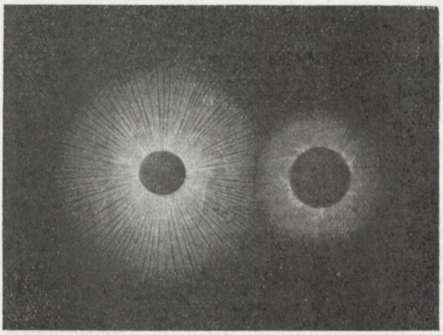

Fig. 15. Negative Figure corresponding to Fig. 14.

The size and shape of the L. F. are to a remarkably high

degree independent of the nature of the insulating plate and of the condition of its surface. Plates of glass, quartz, ebonite, and pitch give exactly the same figures. As shown by E. W. BLAKE (1870)[1] L. F. may also be obtained on pitch which is heated to its melting point. Even on a water surface the regular figures may be observed, as pointed out by E. REITLINGER (1860)[1]. The shape and character of the figures is exactly the same whether the plate is powdered before or after the discharge has taken place. The dust figures and the photographic figures have also the same shape and character, the entire difference being that the dust figures are somewhat coarser and consequently do not show such fine details as the photographic ones.

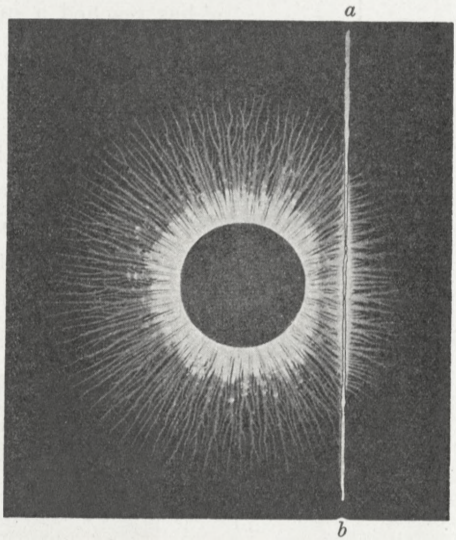

Fig. 16. Positive Figure. *ab* Screen of *a* 0.77 mm. Glassplate cemented to the Film of the Photographic Plate. (Air; $p = 760$; $l = 5$; $D = 17$; $d_0 = 1.4$; $m = 1$).

If the conductivity of the surface of the insulating plate is too great, the intensity of the electric field along the plate will not attain the necessary high value and no LICHTENBERG figure will appear, but the discharge will take some other form. In as far as the conductivity does not attain such a high value, the LICHTENBERG figures are entirely independent of the state of ionization at the surface of the plate. This has been shown in many ways of which I shall only mention the following.

A spark gap g' was inserted between R_1 and the point a (see Fig. 10), and a condenser C' between the point b and a point between g' and R_1. C' had a greater capacity than C. When the p. d. across g' has reached a sufficiently high value a spark passes in g', the condenser C begins to be charged and a spark passes through g causing a Lichtenberg figure to be formed on the plate P. The spark in g' precedes the Lichtenberg figure by about 1×10^{-6} second. The spark gap g' was placed above and at some distance from the photographic plate, a perforated screen being inserted between them. The distance between the spark and the photographic plate was varied within wide limits; with the greatest distance the blackening of the exposed parts of the plate could barely be seen, while with the shortest distance the exposed spots were completely opaque. In all cases the size, shape, and character of the figures were the same in the exposed and in the unexposed parts of the figures, and no peculiarity was to be seen at the places where the Lichtenberg figures passed from an exposed to an unexposed spot or vice versa.

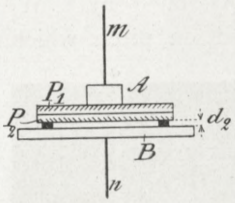

Fig. 17. Arrangement for Primary and Secondary Figures.

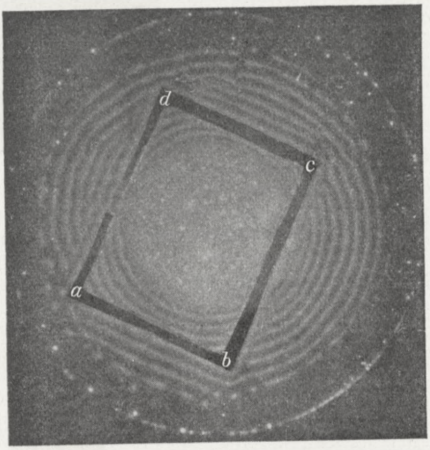

Fig. 18. Negative Secondary Figure corresponding to Primary in Fig. 19. *abcd* rectangular Frame of Mica cut between *a* and *d*. Thickness about 0.2 mm.

Other experiments were carried out with ionization pro-

duced by γ-rays from radium enclosed in a platinum tube. The arrangement for the producing of the LICHTENBERG figures was the normal one shown in Fig. 10, and the radium tube was placed on a sheet of ebonite at a distance of from 2 to 6 mm. above the photographic plate. The ebonite plate was 1 mm. thick and had a hole just below the tube. The plate was exposed to the γ-rays for 15 to 60 seconds before the Lichtenberg discharge took place, and the exposed spots were accordingly more or less blackened. Many experiments were made, but it was in no case possible to ascertain any influence whatever of these spots of ionization upon the Lichtenberg figures, whether they were positive or negative.

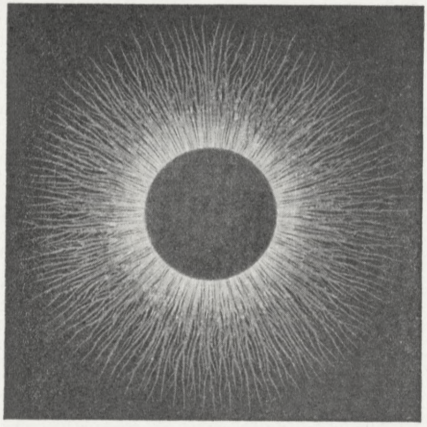

Fig. 19. Positive Primary Figure corresponding to Secondary in Fig. 18. (Air; $p = 760$; $l = 7$; $D = 24$; $d_0 = 2 \times 1.4$; $m = 0.8$).

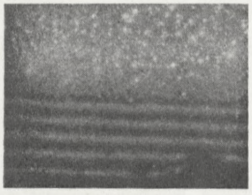

Fig. 20. Part of Negative Secondary Figure. The Electrode had a straight Edge and covered the homogeneous Part of the Figure. ($d_2 = 0.2$ mm).

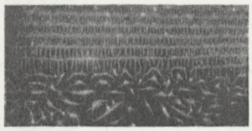

Fig. 21. Part of Positive Secondary Figure starting from below a straight Edge *aa* of the Upper Electrode ($d_2 = 0.2$ mm).

On the other hand we have also tried to remove all chance

ions from the surface on which the Lichtenberg figure is formed. In order to do this a ring-shaped electrode was placed on the photographic plate concentric with the electrode A (see Fig. 10), and a battery in series with an induction coil was inserted between A and the ring electrode. The E. M. F. of the battery was varied within wide limits and any natural ionization was, no doubt, either completely removed or at least greatly reduced. The discharges took place with the battery inserted, and the Lichtenberg figures thus formed were in no way different from the others.

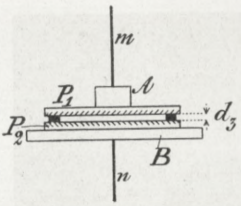

Fig. 22. Arrangement for Tertiary Figures.

It appears from these and other experiments that the Lichtenberg figures within extremely wide limits are independent of the state of ionization at the surface of the plate. These figures are thus in a very high degree independent of the nature of the plate and the mechanical and physical condition of its surface. We shall later on see that size, shape, and character of the Lichtenberg figures depends almost exclusively on the nature and pressure of the surrounding gas.

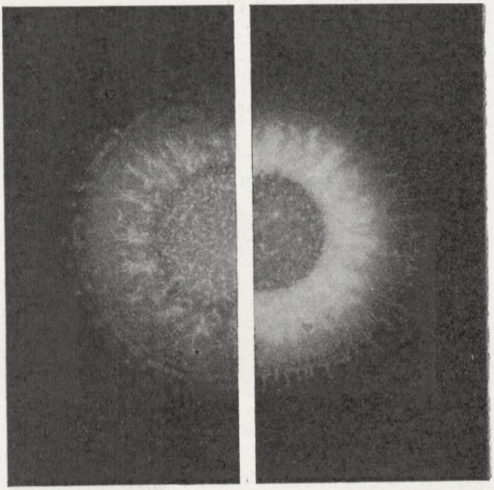
a *b*

Fig. 23. *a* Lower and *b* Upper Tertiary Figure for Negative Discharge. (Air; $p = 760$; $l = 8$; $D = 17.5$; $d_3 = 0.1$; $m = 1$).

2. We have so far only considered figures which start from the small electrode. W. G. ARMSTRONG and H. STROUD

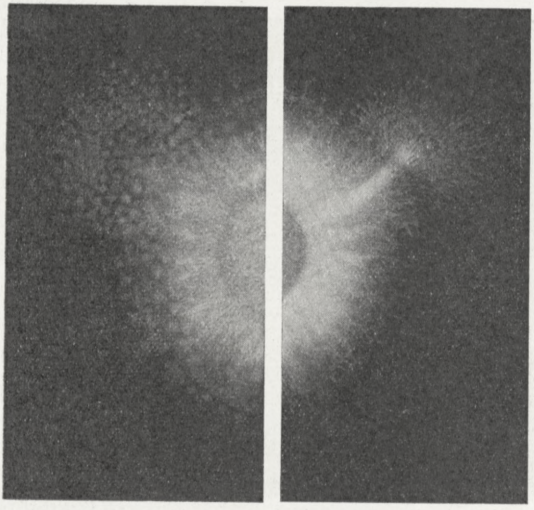

a *b*

Fig. 24. *a* Lower and *b* Upper Tertiary Figure for Negative Discharge. (Air; $p = 760$; $l = 8$; $D = 17{,}5$; $d_3 = 0.1$; $m = 1$).

(1899)[1] and S. MIKOLA (1917)[1] have shown that very remarkable figures may be obtained in front of the great electrode B on a sensitive film at a little distance (P_2 Fig. 17). S. MIKOLA calls these secondary figures and those formed from the electrode A primary Lichtenberg figures. A secondary figure is shown in Fig. 18, while Fig. 19 shows the corresponding primary figure. Parts of secondary figures are also shown in Fig. 20 and 21. We call these secondary figures negative (positive) when the simultaneous primary figure is positive (negative).

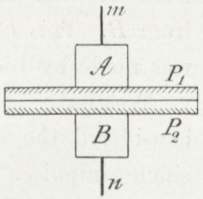

Fig. 25. Arrangement for Simultaneous Positive and Negative Figures.

A third kind of figures are obtained if two photographic plates are placed between the electrodes with the sensitive

films against each other. We call these tertiary figures. If the distance d_3 (see Fig. 22) between the films is small, very remarkable and finely shaped figures may be obtained. Examples of such figures are shown in Figs. 23 and 24. The explanation of these figures will hardly offer any greater difficulty when the problems of the primary and secondary Lichtenberg figures have been solved.

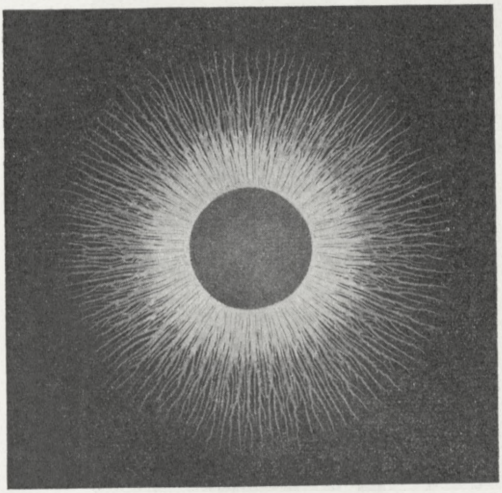

Fig. 26. Positive Figure. (N_2; $p = 760$; $l = 5$; $D = 17.5$; $d_0 = 1.4$; $m = 1$).

If the two electrodes A and B are of approximately the same size (see Fig. 25) there is simultaneously formed two primary figures of opposite polarity, say a positive from A and a negative from B. This observation was made by Lichtenberg.

We have so far only considered the effect of a single impulse. The discharge of the condenser C through the circuit $gmABnb$ will generally, however, be oscillatory (see Fig. 10). The Lichtenberg gap APB

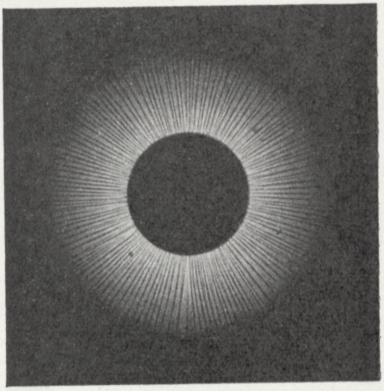

Fig. 27. Negative Figure. (N_2; $p = 760$; $D = 17.5$; $d_0 = 1.4$; $m = 1$).

forms a small condenser of a capacity C'' which increases as the size of the figure starting from A increases. The period T of the oscillation is determined by

$$T = 2\pi \sqrt{L_0 \frac{CC''}{C + C''}},$$

where L_0 is the coefficient of selfinduction of the circuit *CagsqbC* and C the capacity of the condenser C.

The damping of these oscillations depends upon the resistance of the wires, the dielectric losses in the condensers, the loss in the spark gap, but especially upon the losses caused by the shunt R and by the LICHTENBERG discharge itself. In cases where the combined effect of these losses does not give a sufficiently high damping the first impulse will, half a period later, be followed by an impulse of opposite polarity, and this latter impulse will create a new discharge superposed on the previous one. Without the shunt R (see Fig. 10) the damping of a positive discharge at atmospheric pressure will generally be so small that the effect of the succeeding negative impulse is rather great. The inner part of the positive figure is then covered by the following negative discharge as shown in Figs. 12, 16, 19, and 26. It is seen that this negative discharge mainly follows the paths of the preceeding positive one. By

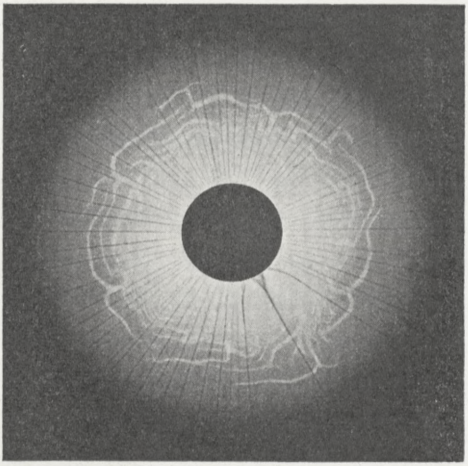

Fig. 28. Negative Figure. (93 % N_2 + 1 % O_2; $p = 150$; $D = 17.5$; $d = 1.4$; $m = 0.8$).

use of a suitable shunt the negative impulse may be sufficiently reduced; the positive figure then appears pure as in Fig. 6.

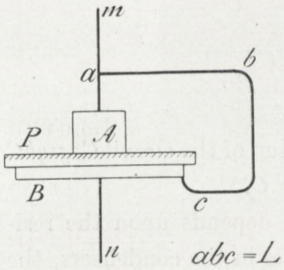

Fig. 29. Arrangement for Oscillating Discharges.

At lower pressure the positive figures will often be pure even if no shunt is used. The negative discharge at atmospheric pressure is generally so highly damped that the succeeding positive impulse is without any appreciable effect; the negative figure therefore generally appears pure as in Figs. 7 and 27. At lower pressures the negative discharge is apparently less damped and the succeeding positive impulse therefore able to effect a positive discharge superposed on the preceeding negative one. Fig. 28 shows a positive discharge of this kind; its appearance is very remarkable, but the further discussion of this question will be taken up later on.

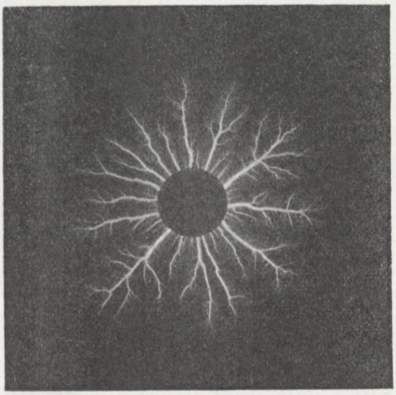

Fig. 30. Oscillating Discharge, first Half-wave Positive. $L = 133$ cm. (Air: $p = 760$; $l = 10$; $D = 9.5$; $d_0 = 1.3$; $m = 1$).

If the L. G. is shunted by a wire *abc* (see Figs. 29 and 10) the period of the circuit *CgmabcnqbC* is increased and the damping reduced so much that an ordinary, slightly damped oscillation is created in this circuit when a spark passes at *g*. In this case each of a number of succeeding half-waves of opposite polarity will cause discharges to take place, and the figure made during the first discharge is overlapped by the

succeeding figures and it is rather indifferent whether the first discharge was positive or negative. Fig. 30 shows a "positive" figure of this kind and Fig. 31 a "negative" one, but there is hardly any difference between them. We have not found opportunity to investigate the properties of these figures.

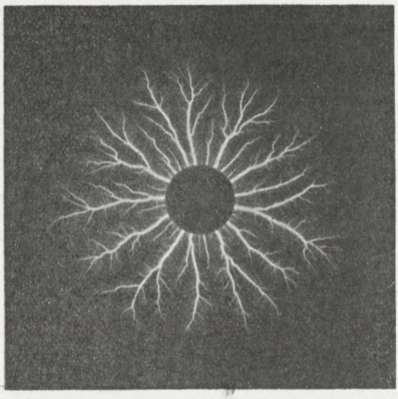

Fig. 31. As Fig. 30, but first Half-wave Negative.

Chapter III.

General Features of the Lichtenberg Figures.

a. Negative Figures.

1. General Character of the Negative Figures. With the exception of some thin dark lines which we shall consider later on, the pure negative figure appears as a white disk with nearly equal brightness over the whole area, except the external boundary though, where the brightness gradually dies away (see Figs. 7, 27, and 28). In all works dealing with LICHTENBERG dust figures the negative figures are only characterized by their external boundaries, being marked by a strong dust ring, generally appearing just outside the negative disk (see Fig. 3). The above mentioned dark lines are so fine that they are unable to manifest themselves clearly with the dust method.

Using the photographic method it is clearly seen that the negative figure is broken up in separate parts by a number

of dark lines (see Figs. 7, 27, and 28). We will call each of these bright parts a negative flow or stream. The width of the negative flows varies in the same figure within wide limits, while the dark lines are very nearly all of the same width. The boundary between the dark lines and the negative streams is, however, not very sharply defined, the transition from the white parts to the dark ones being more or less gradual, and there is an uncertainity of about $\pm$ 0.005 mm. in the determination of the boundary line.

The mean width of the negative flows in Fig. 27 (measured at a distance of 8 mm. from the electrode) is 0.68 mm., the broadest being 1.10 mm. and the narrowest 0.18 mm. wide. In other instances the variation is even greater (see f. inst. Fig. 28). Strongly contrasted with this is the great constancy in the width of the dark lines*.

The mean value of the width of 16 consecutive dark lines in Fig. 27 was 0.095 mm., and the greatest deviation $\pm$ 0.009 mm. The width of the different dark lines is thus at least nearly constant, and for the same line its width is nearly the same over its whole length, with the exception of the part in the neighbourhood of the electrode where the dark lines are sometimes much broader (see f. inst Fig. 28). We shall later on return to this point.

The width of the dark lines is apparently independent of the spark length and of the size of the electrode. To show this we quote in Table 1 some figures obtained in air at atmospheric pressure.

For short spark lengths it is difficult to measure the width of the dark lines. The figures in the table give the limits within which the width was estimated to fall.

The mean value of the width of the negative flows also

* This constancy of the width of the dark lines seems to have escaped the attention of S. Mikola, probably because he preferably used rather thick plates, with which these lines are broader and less regular.

Table 1. Width of Dark Lines in Air
(p = 760 mm. hg).

Length of spark l in mm.	1.	2.	3.	5.	7.	9.
Width of dark lines in mm. electrode: D = 40 mm.	0.09—0.11	0.09—0.11	0.09—0.11	0.92	0.10	0.092
electrode: point	0.09—0.11				0.10	0.091

seems to be independent of the spark length, in other words, the number of negative flows is nearly independent of the spark length.

The width of the dark lines depends also very little on the nature of the gas, as shown by the following figures.

Table 2.

		Mean Value of Width of Dark Lines	Negative Streams
Air	p = 760 mm. hg.....	0.095 mm.	0.68 mm.
N_2	—	0.095 -	0.68 -
H_2	—	0.100 -	0.58 -
CO_2 (from flask)	—	0.11 -	1.25 -
O_2 (—)	—	0.18 -	0.50 -

With the exception of oxygen the width of the dark lines is practically the same for all gases investigated. Also in other respects oxygen behaves differently from air, nitrogen, hydrogen and carbon dioxide. The average width of the negative flows is also nearly the same with the exception of carbon dioxide for which gas it is nearly twice as great as for the other four gases.

In Fig .32 are shown some enlarged photographs* of parts of negative figures in different gases. It is seen that there is no great difference between figures in nitrogen (Fig. 32 a), air (h), hydrogen (d), and carbon dioxide (f). While the lines are straight in the three first mentioned gases, they are, however, somewhat bent in carbon dioxide. In oxygen (e) the figures are not so regular as in the other gases.

* The width of the dark lines has been measured directly on the LICHTENBERG plates. On copies the dark lines will often appear broader or thinner according to circumstances. Fig. 32 is therefore not to be used for a measurement of the width of the dark lines.

The width of the dark lines and the flows increases with decreasing pressure, this increase being especially pro-

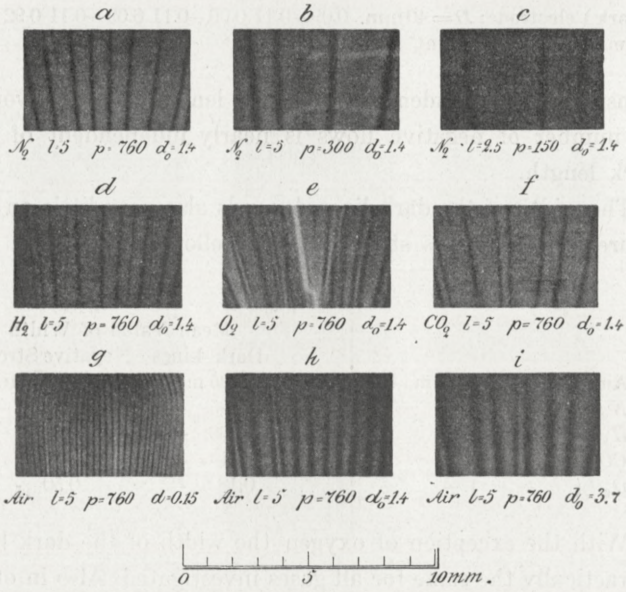

Fig. 32. Parts of Negative Figures in various Gases and at various Pressures.

nounced in case of the flows as shown in the following table.

Table 3. Width of Dark Lines and Negative Flows for Different Pressures.

Gas: — Nitrogen (from steel flask, 93 % N_2 + 7 % O_2).

Pressure	760	300	150	75 mm. hg.
Width of dark lines	0.095	0.154	0.173	0.25—0.30 mm
Average width of negative flows.	0.68	0.93	1.6	2.8 mm.
Maximum — — ..	1.10	4.5	12.0	11.0 -
Minimum — — ..	0.18	0.3	1.4	1.0 -

The influence of varying pressure in the case of nitrogen is shown in Fig. 32 a, b, c.

The width of the dark lines and the average width of the negative flows decreases with decreasing thickness of the photographic plate as shown in the following table.

Table 4. Width of Dark Lines and Negative Flows for Different Thicknesses of Plate.

Thickness d_0 of plate P (see Fig. 10)...	0.15	1.4	3.7 mm.
Width of dark lines	0.055	0 10	0 25 mm.
Average width of negative flows.....	0.18	0.68	0.82 -

This feature is illustrated by Fig. 32 g,h,i. When d_0 is small both the dark lines and the negative flows are very narrow. The greater the value of d_0 the greater is also the width of the dark lines while there seems to be a limit value of the average width of the negative flows. With great value of d_0 the constancy of the width of the dark lines is not so pronounced and the whole figure becomes less regular.

On very thin plates the dark lines have a tendency to be bent but are otherwise very regular.

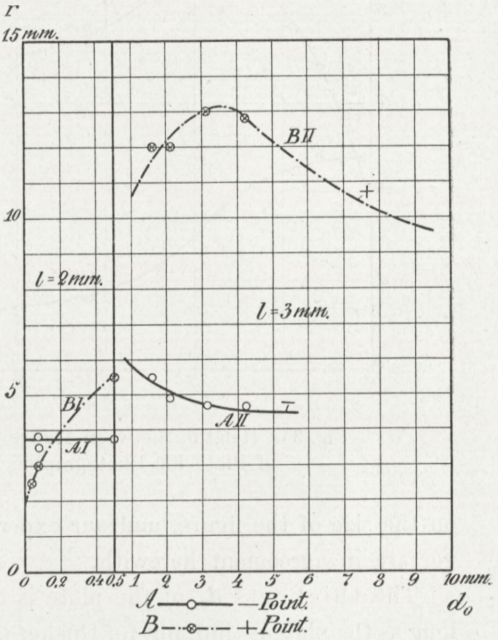

Fig. 33. Effect of Thickness of Plate (d_0) on the Range (r) of Dust Figures.

2. Size or Range of the Negative Figures. The size may be measured in different ways; as the size we shall

take the range or the length r of the negative flow reckoned from the electrode to the outermost end. It is to be expected that the size will be dependent upon a good many things. We shall in the following investigate the influence of some of the most important of these factors.

W. v. Bezold (1871)[4] proved that the dielectric constant of the plate P (see Fig. 10) has little or no influence

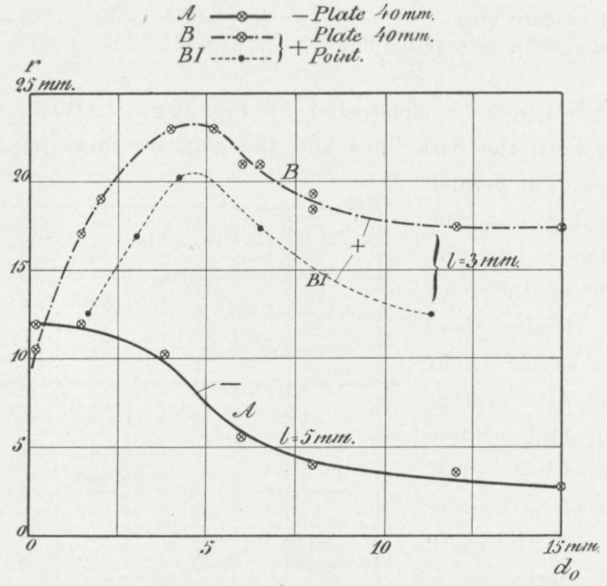

Fig. 34. Relation between Range and Thickness of Plate for Photographic Figures.

on the size of the figure, and our experiments, as far as they go, are in agreement herewith.

The thickness d_0 of the plate is of little importance so long as the plate is thin, but for thicker plates there is a marked decrease in size with increasing thickness. This is evident from Fig. 33 which shows the results of W. v. Bezold's measurement for dust figures, and Fig. 34, containing some of our results for photographic Lichtenberg figures. For

very great values of d_0 the range very slowly approaches the value of r corresponding to $d = \infty$.

The influence of the spark length was investigated by W. v. Bezold (1871)[4], S. Mikola (1917) and others. Bezold's

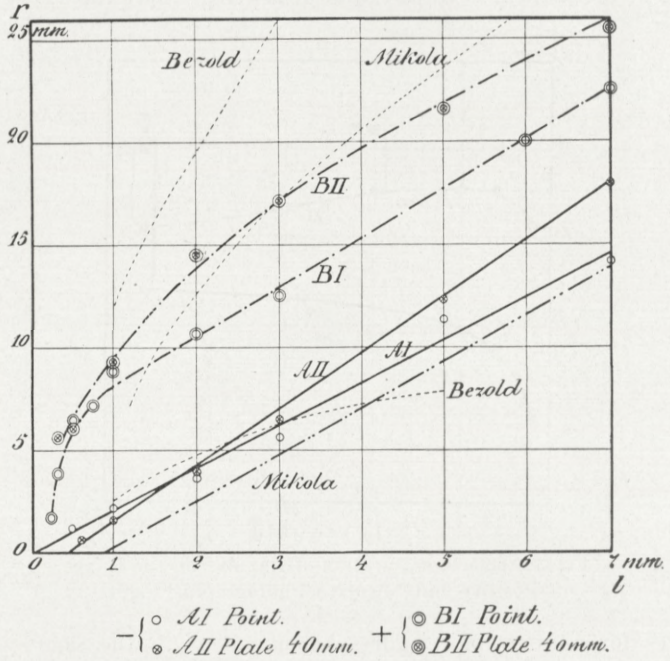

Fig. 35. Effect of Spark Length (l) on the Range (r) of Positive and Negative Figures. (Air; $p = 760$; Bezold's values are for Dust Figures, the others refer to Photographic Figures. $d_0 = 1.4$ in A and B-curves, by Mikola about 3 to 4 mm. D is about 20 mm. by Mikola).

and Mikola's results are shown in the lower part of Fig. 35 which also contains the results of our measurements. Both Mikola's and our own measurements give a linear relation between spark length and size, while v. Bezold's curve is bent with the concavity against the l-axis. v. Bezold's results refer to dust figures, and the size of negative dust

figures is generally taken as the radius of the dust ring enclosing the negative figure. Such rings do not appear in the photographic Lichtenberg figures, and it is therefore difficult to compare the size of these two kinds of figures. It ought to be mentioned, however, that at lower pressure the (l, r)-cur-

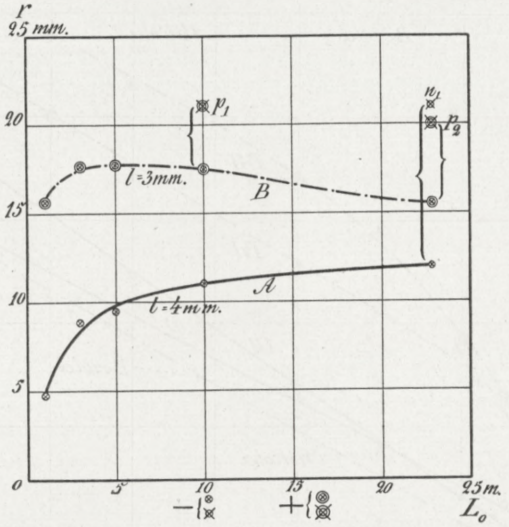

Fig. 36. Effect of Duration of Impulse on the Range of Positive and Negative Photographic Figures.

ves for photographic figures become bent in the same way as v. Bezold's curve.

For point-electrode the (l, r)-line seems to pass through the origin (AI in Fig. 35), while the (l, r)-lines for greater electrodes starts from the l-axis to the right of the origin (AII), and the more so the greater the diameter of the electrode and the thickness of the plate is. These results are in complete agreement with the investigations of M. Toepler[1].

Another point to be noted is that the angle, which the (l, r)-line makes with the l-axis, increases with increasing size of the electrode, being smallest for a point-electrode. S. Mikola generally uses much thicker plates than we do, and

his electrode seems to have had a diameter of about 20 mms., intermediate between our point-electrode (*AI*) and plate-electrode (*AII*), which had a diameter of 40 mms. Considering all these points it appears from Fig. 35 that the agreement between MIKOLA's measurements and ours is very good.

Effect of duration of the impulse on the size of the negative figure. In order to investigate this point we have altered the lengths of the wires k_2s and bq (Fig. 10) keeping all other circumstances as far as possible constant. In Fig. 36 we have plotted the value of r as a function of the length L_0 of each of the wires k_2s and bq. For short wires (up to about 10 metres) r is very nearly proportional to the square root of L_0, for longer wires the increase of r is very slow. But here a new phenomenon sets in, consisting in the formation of fan shaped extensions outside or nearly outside the range of the normal figure (see Fig. 37). The greatest lengths of these are in Fig. 36 marked n_1. This form of discharge is very similar to that caused by too high tension and both are closely connected with the sliding sparks investigated by M. TOEPLER.

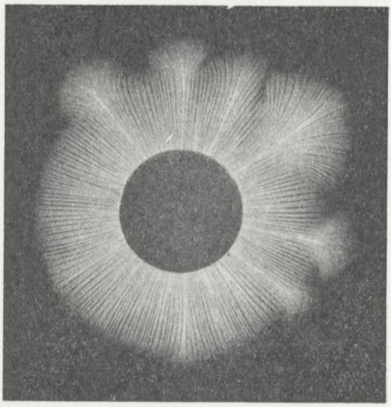

Fig. 37. Negative Figure. (Wire $k_2s = bq = 23$ m., see Fig. 10. (Air; $p = 760$; $l = 4$; $D = 17.5$; $d_0 = 1.4$; $m = 1$).

Effect of gas pressure on the range. W. v. BEZOLD (1871)[4] found that

$$p \cdot r = \text{constant},$$

while S. MIKOLA (1917) expresses the results of his measurements in the empirical formula:

$$r = \frac{r_0}{(p+k)^{3/2}},$$

r_0 and k being constants.

The full curve in Fig. 38 shows the results of our measurements and in the same figure curves are drawn corresponding to Bezold's and Mikola's formulae. The constant in the first is chosen so that Bezold's formula agrees with our

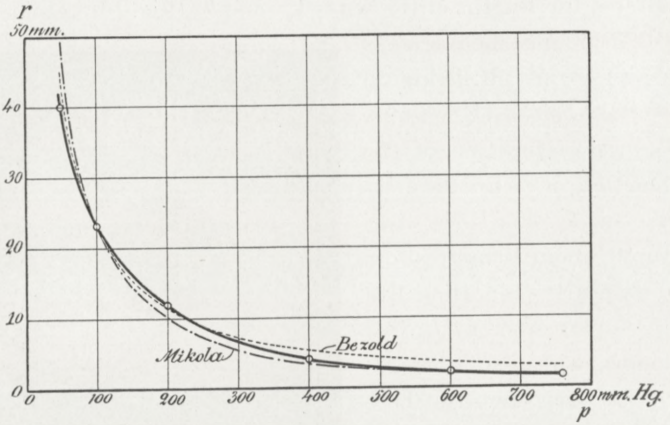

Fig. 38. Relation between Gas Pressure and Range of the Negative Figures. (Air; $l = 2$; $D = 10$; $d_0 = 1.4$).

value of r for $p = 100$ mm. hg., while r_0 and k in Mikola's formula are given such values that his curve agrees with ours for $p = 100$ and $p = 600$ mm. hg.

The differences between the three curves are not great, and the measurements cannot be made sufficiently accurate to determine with certainty which of the two curves is the best representative of our experiments. There is, however, hardly any doubt that the product $p \cdot r$ increases with decreasing pressure.

The dependence of the range on the nature of the gas has not yet been sufficiently investigated. We shall therefore only quote the results of a few provisional measurements.

Table 5. Range of Negative Figures in Various Gases. ($l = 5$ mm.; $p = 760$ mm. hg.).

Gas:	Range:
Air	13.0 mm.
Nitrogen from steel flask (93 % $N_2 + 7$ % O_2)	13.0 -
Hydrogen —	13.5 -
Oxygen —	8.5 -
Carbon dioxide —	10.0 -

b. Positive Figures.

1. General Character of the Positive Figures. The positive figures will later on be subjected to a more detailed investigation, we shall therefore at present only consider their general appearance.

The positive figures consist of sharply defined stems or trunks with short, well defined branches or offshoots, see Figs. 6, 14, 16, and 19. The appearance of the figures, and especially the ramification, depends on the nature of the gas, and we shall later on return to this point; for the present we shall only deal with some general features of positive figures in atmospheric air or in nitrogen.

Effect of gas pressure on the appearance of the figures. It has been found that the number of branches per centimetre of trunks is proportional to the pressure. To illustrate this point some of our results are quoted in Table 6.

Table 6. Effect of Gas Pressure on the Number of Branches. Nitrogen from steel flask (93 % $N_2 + 7$ % O_2).

Pressure p mm. hg.	Number N of branches on 1 cm. of trunk	$100 \frac{N}{p}$
760	7.7	1.0
300	3.0	1.0
150	1.14	0.76
75	0.64	0.85
34	0.36	1.1
	Mean value..	0.94

The values of N quoted in the table are mean values for at least 10 different trunks, and there is, and necessarily must be, a rather great uncertainty in the determination of N. The figures in Table 6, however, strongly support the view that the average number of branches per centimetre of trunk is proportional to the pressure.

We have further found that the product of gas pressure and width of trunks is constant. This relation, however, only holds good at the free ends of the trunks; close to the electrode, where the different trunks cannot find sufficient space to develop, this relation does not hold good and cannot be expected to do so. The width of the trunks generally decreases from the electrode outwards, and the width ought to be measured in corresponding points. As such we have taken points whose distance from the top of the trunks is inversely proportional to the gas pressure. The results of such a series of measurements are quoted in the following table.

Table 7. Effect of Gas Pressure on the Width of the Trunks. Nitrogen from steel flask (93 % N_2 + 7 % O_2).

Pressure p mm. hg.	Width of trunks t mm.	Distance from test point to top of trunk mm.	$p \cdot t$
760	0.12	0.5	91
300	0 29	1.3	87
150	0.59	2 6	89
75	1.42	5 2	106
34	3.60	11.0	119
		Mean value..	98

In order to illustrate this point we have also taken a series of microphotographs of the top end of trunks in the same gas but at different pressures, making the magnification proportional

to the pressure. Fig. 39 shows such a series of microphotographs. It appears from Table 7 and Fig. 39 that the product of gas pressure and width of trunks or branches is very nearly constant in the interval from atmospheric pressure down to about 75 mm. hg. For pressures below 75 mm. hg. the width of the trunks is greater than according to this rule.

2. The range of the positive figures is mainly dependent upon the same physical constants as the range of the

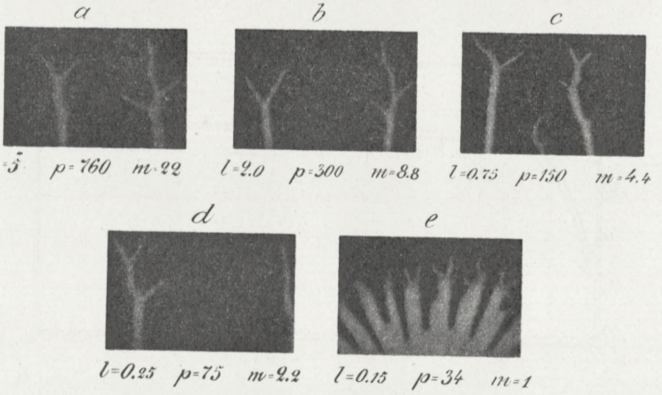

Fig. 39. Microphotographs of Top Ends of Trunks, the Magnification being equal to $\frac{p}{34}$.

negative figures but the influences of some of these constants show very characteristical differences in the two cases. The range r is, as shown by W. v. Bezold (1871)[4], independent of the value of the dielectric constant for isotropic plates. For crystalline plates the range may be different in different directions, a fact first discovered by E. Wiedemann (1849)[1]. We shall, however, in this paper confine ourselves to the discussion of isotropic plates.

The range depends very much on the thickness of the plate. W. v. Bezold's results for dust figures at atmospheric

pressure are indicated in Fig. 33, while Fig. 34 shows some of our measurements for photographic Lichtenberg figures. An example of a (d_0,r)-curve at lower pressure is shown in Fig. 40. While the range of the negative figures attains its maximum value for very small values of d_0 (see Fig. 33 and 34), the range of the positive figure on the contrary is very small for small values of d_0, and attains large values for greater values of d_0. At atmospheric pressure the range is maximum

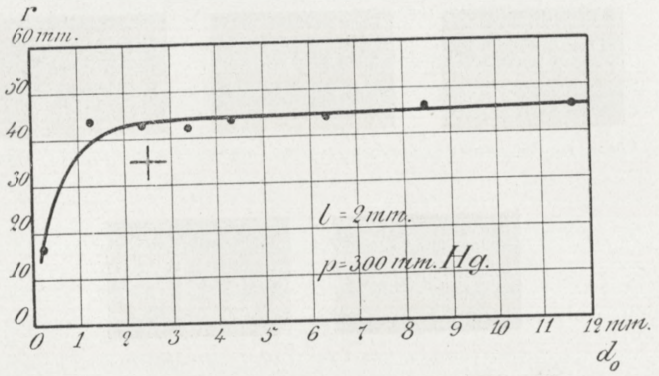

Fig. 40. Effect of Thickness of Plate on the Range of the Positive Figure. (Air; $p = 300$; $l = 2$; $d_0 = 1.4$).

tor d_0 about 5 mm.; at lower pressure the range seems to be maximum for $d_0 = \infty$ (see Fig. 40.).

The relation between range and length of spark for air at atmospheric pressure is shown in Fig. 35. W. v. Bezold's measurements refer to dust figures, S. Mikola's and ours to photographic figures. The agreement between the three sets of measurements is not very good. The rather great ranges found by W. v. Bezold are probably due to the fact that his voltages varied too rapidly, the sparking voltages thereby attaining too high values. The difference between S. Mikola's and our measurements is — partially at least — due to difference in the thicknesses of the plates, by Mikola about

3 or 4 mm. in our experiments about 1.4 mm. For small spark lengths the character of the (l,r)-curves differs very much for positive and negative figures. While the (l,r)-curves for negative figures approximate straight lines, which for point electrodes apparently start from the origin, the corresponding curves for positive figures all start from some points of the positive l-axis and in a direction approximately normal to this axis; this is even true for point electrodes. For greater spark lengths the curves bend towards the l-axis and become approximately straight and parallel to the corresponding lines for negative figures.

S. Mikola gives the following formulae for the range of the positive and negative figures

$$r = a_1 \sqrt{V - V_0} \quad \text{for positive figures} \qquad (a)$$

and

$$r = a_2 (V - V_0) \quad \text{for negative figures.} \qquad (b)$$

V being the actual spark potential and V_0 the smallest P. D. capable of producing a figure.

According to Mikola V_0 has the same value in (a) and (b), that is to say that the positive and negative (l,r)-curves start from the same point. This is, however, as we have seen, only true in special cases. With point electrodes the negative (l,r)-curve always seems to start from the origin while the positive curve starts from a positive point of the l-axis. The following experiment is also in accordance with this view. A point electrode suddenly connected to a P. D. of 440 volts gave small but well defined negative Lichtenberg figures at atmospheric pressure. Of a positive figure no trace was obtained even with 730 volts, the largest constant P. D. at our disposal. The formulae (a) and (b) are thus no doubt only approximate ones and can only be used within certain limits, and V_0 will in general have different values in (a) and (b).

The effect of the duration of the impulse on

the range was tested in the same way as the similar question for negative figures, and the results are plotted in Fig. 36. The range of the positive figures seems to be rather independent of the duration of the impulse, while for negative figures the range is approximately proportional to this duration. A positive figure of normal size and character appears when the P. D. across the L. G. has reached a certain value even if the P. D. is only kept on during an extremely short time.

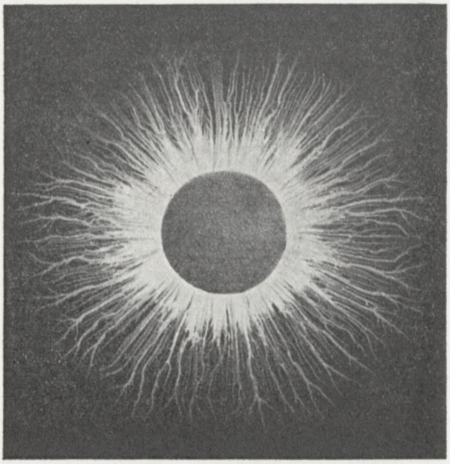

Fig. 41. Positive Figure. (Wire $k_2 s = bq = 23$ m.; Air; $p = 760$; $l = 3$; $D = 17.5$; $d_0 = 1.4$; $m = 1$).

If the P. D. is applied during a relatively long time, a new discharge takes place, the range of which is indicated by points marked p_1 and p_2 in Fig. 36. In so far there is a close analogy between the behaviour of the positive and negative figures. But while the negative fanshaped discharges seem to start from the ends of individual small sparks (see Fig. 37), the second positive discharge seems to have exactly the same character as the first one (see Fig. 41). The only difference between the first and second discharge seems to be that the trunks of the last are confined to the free spaces between the trunks of the first discharge. The trunks of the second discharge are therefore comparatively narrow in the neighbourhood of the electrode and expand as soon as they find sufficient space to do so. (Some of the details mentioned have been lost in the reproduction of Figs. 37 and 40).

W. v. Bezold (1871)[4] and S. Mikola (1917)[1] investigated how the range of the positive figures depends upon the pressure in the gas.

v. Bezold found the following formula

$$r = \frac{a_1}{p},$$

while S. Mikola found that

$$r = \frac{a_2}{(p + k)^{3/2}}$$

was in better agreement with his measurements. a_1, a_2, and k are constants.

One of our series of measurements is plotted in Fig. 42. It does not agree with any of the above formulae; but with suitable values of the constants the discrepancies are only small in both cases. Both formulae are to be considered as empirical and, as v. Bezold's only contains one arbitrary constant and Mikola's two, it would be natural to prefer the first of the two formulae, at least until further evidence is available.

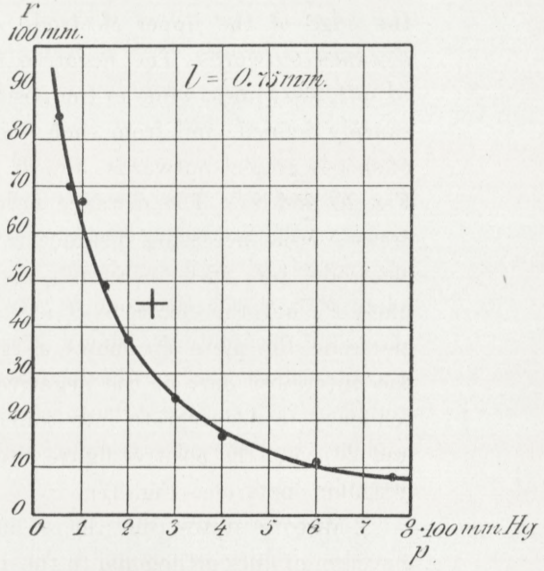

Fig. 42. Relation between Gas Pressure and Range of Positive Figure. (Air; $l = 0.75$; $d_0 = 1.4$).

The range depends also upon the nature of the gas, but we have not yet made any definite measurements. The following table contains some of our provisional results.

Table 8. Ranges of Positive Figures in Various Gases.
(l = 5 mm.; p = 760 mm. hg.).

Gas:	Range:
Air	23 mm.
Nitrogen from steel flask (93 % N_2 + 7 % O_2)	23 -
Hydrogen —	28 -
Oxygen — (the positive figure is very faint)	20 -
Carbon dioxide —	11 -

c. Secondary Figures.

1. General Features. These figures have been observed by W. G. Armstrong and H. Stroud (1899, plates III and IV of Supplement), and reproductions of very fine specimens of them are to be found in S. Mikola's paper (1917). The secondary figures start on the plate P_2 (see Fig.17) a little outside the edge of the upper electrode A, and continue for some distance outwards. The negative figures consist of a series of soft, hazy lines, while in the positive ones the lines are more sharply defined, and from each line a great number of sharp offshoots project outwards, almost reaching the next line (see Fig. 20 and 21). The distance between consecutive lines increases with increasing distance from the edge of the upper electrode and with increasing distance between the lower plate P_2 and the electrode B (see Fig. 17). Below the upper electrode the plate P_2 shows a rather uniform light, while the outermost part of the negative secondary figure shows a tendency to disintegrate into round, hazy spots (see Figs. 18 and 20), and the positive figure into sharply defined but very irregular spots (see Fig. 21).

S. Mikola states that the secondary figure always forms a system of lines orthogonal to the discharge lines of the simultaneous primary figure. This is, however, not always true, as an inspection of Figs. 18 and 19 will prove. Fig. 18 shows a secondary and Fig. 19 the simultaneous primary figure. The plate P_2 rested on a rectangular frame *abcd* of mica which had no influence whatever on the primary figure (Fig.

19) but caused very marked alterations in the lines of the secondary figure (Fig. 18). A comparison between the two figures shows that the two sets of lines are not always orthogonal to each other, but it shows also that there is some tendency towards this orthogonality.

Chapter IV.

Velocity of the Positive and Negative Lichtenberg Discharge.

1. Method of Measurement. For the elucidation of the origination of these figures it is of great importance to

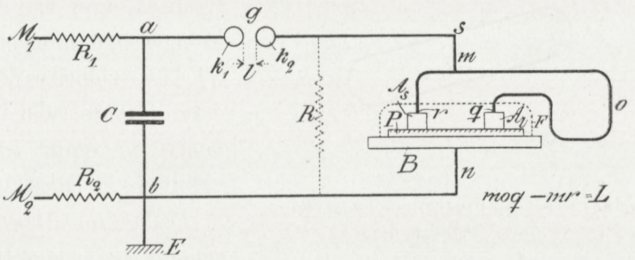

Fig. 43. Circuit Connections in Velocity Measurements.

determine the manner in which they attain their final shape and size. The figures may possibly originate in either of two ways: They may almost at once attain their final shape and size while the intensity increases during the time it takes to form the figure; or the figures may spread out from the electrode attaining, more or less, the final intensity as far as the discharge has reached while there is no alteration outside the instantaneous boundary of the figure. In the latter case the velocity of the spreading out becomes of great interest, and if this velocity can be determined, it is thereby proved that the figures originate by spreading out from the electrodes.

In the following we shall describe a method for the measure-

ments of this velocity, together with the results of a number of such measurements under different conditions and for different gases.

The main principles of the measurements are indicated in Figs. 43 and 44, of which the first shows the diagram of connections and the second the form and the position of the two upper electrodes used in the measurements. When a spark passes through g, an electric wave starts herefrom and travels from k_2 along the wire leading to m. Here it parts in two separate waves, one running along the wire mr to the electrode A_s and the other along moq to the electrode A_l. The velocity of the wave fronts will very nearly be equal to the velocity of light $v = 3 \times 10^{10}$, and if the wire moq is L cm. longer than mr, the wave travelling along moq will reach A_l τ seconds later than the other wave reaches A_s, where $\tau = \frac{L}{v}$.

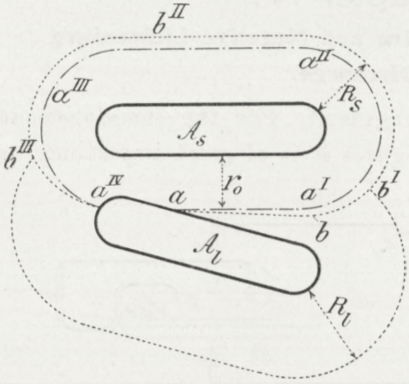

Fig. 44. Form and Position of Eleotrodes in Velocity Measurements.

Both electrodes being alike, their potentials will increase in the same manner, the only difference being that the potential of A_l lags τ seconds behind that of A_s. The discharge will therefor start τ seconds later from A_l than from A_s, and if the discharge travels a distance r_0 cm. from A_s before the electric wave reaches A_l, the mean velocity u of the discharge is determined by

$$u = \frac{r_0}{\tau} = \frac{r_0}{L} v = \frac{r_0}{L} \cdot 3 \cdot 10^{10} \text{ cm/sec.}$$

It is of great importance to chose the shape, size, and positions of A_s and A_l in such a manner that the value of r_0 may

be determined without ambiguity. Electrodes of the form shown in Fig. 44, and placed as indicated, have proved to answer very well and have been used in almost all our experiments.

The electrodes are placed in such a way that the shortest distance between them is slightly less than r_0. The discharge from A_s will then have reached A_l at the moment the electric wave through the wire *moq* reaches A_l. The boundary of the discharge from A_s at this moment is in Fig. 44 indicated by $aa^{I}\ a^{II}\ a^{III}\ a^{IV}$. A discharge then starts from A_l while at the same time the discharge from A_s pushes on further outward. The result hereof is, that the two discharges meet in a line abb_1 passing through the point *a*. A part, *ab*, of this line is nearly straight. The behaviour of the discharges at the meeting line is different under different conditions: In positive figures at atmospheric pressure both discharges push beyond the meeting line, the offshoots from one side making their way for some distance into the free spaces on the other side and vice versa. An example hereof is shown in Fig. 45. In this case the meeting line is not very sharp and cannot be determined with any great accuracy. At lower pressure there is either no trespassing

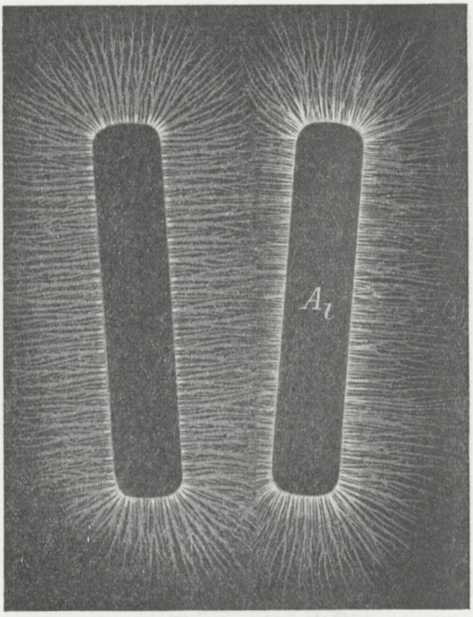

Fig. 45. Positive Velocity Figure. $L = 10$ m. (Air; $p = 300$; $l = 2.5$; $d_0 = 1.4$; $m = 0.8$).

at all or at least only very little, and the meeting line is accordingly very well defined. Examples of such figures are shown in Fig. 46—49. For negative discharges the meeting line is rather well marked at atmospheric pressure (see Fig. 50) while at lower pressures it often becomes less sharp.

As mentioned above the meeting line starts from the point a on A_l (see Fig. 44) reached by the discharge from A_s at the moment the electric impulse reaches the electrode A_l. The first part, ab, is in most cases nearly a straight line making only a small angle with the edge of A_s. That this is so, is easily understood. Before the electric impulse reaches A_l, the electric force in the space between A_s and A_l is due to the charge on A_s and on the area covered by the electric figure which surrounds A_s. As soon as the electric impulse reaches A_l, the electric force exerted by the charge on A_l at points between A_l and aa^{I} will predominate over the force due to the charge on A_s and its figure. As we shall see later on, the velocity increases with increasing force and the figure starting from A_l will therefore spread with greater velocity than that with which the figure belonging to A_s progresses further from the line aa^{I}.

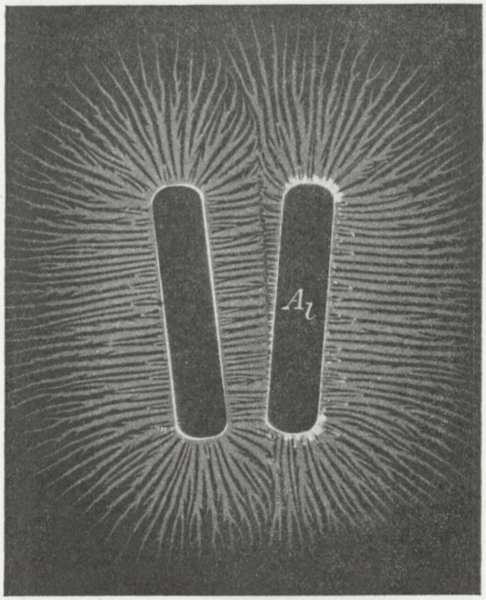

Fig. 46. Positive Velocity Figure. $L = 6$ m. (Air; $p = 300$; $l = 1$; $d_0 = 1.4$; $m = 0.8$).

We have until now supposed the front of the waves travelling along the wires *mr* and *moq* (Fig. 43) to be so steep that the rise in potential at the wave front could be considered as instantaneous. The wave front is, however, in general not so steep, and we will have to consider what difference it makes that the potential of A_s and A_l increases gradually instead of instantaneously. The result of this gradual rise in potential of A_s is that the discharge does not start immediately when the wave reaches A_s but a little later when the potential has attained the necessary value. There will, however, be the same retardation at the electrode A_l, and the measurement of the velocity is so far not affected. But another effect of the gradual rise of potential ought to be considered. During the short interval from the moment the wave front just reaches A_l to the moment the discharge starts from A_l the electric field due to the charge on A_l tends to reduce the

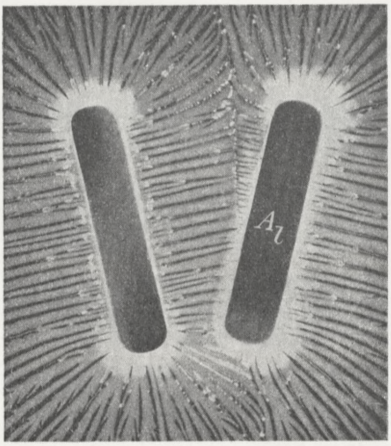

Fig. 47. Part of Positive Velocity Figure. $L = 6$ m. (Air; $p = 300$; $l = 2.5$; $d_0 = 1.4$; $m = 0.8$).

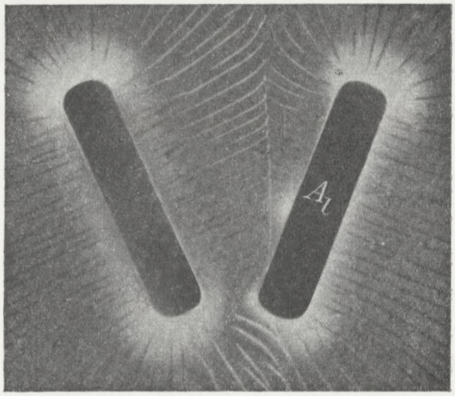

Fig. 48. Part of Positive Velocity Figure. $L = 6$ m. (Air; $p = 150$; $l = 2.8$; $d = 1.4$; $m = 0.8$).

velocity of the discharge from A_s. The result hereof is that the velocity as measured comes out a little too small.

Another possible source of error may conveniently be discussed here. If the discharge does not start immediately when the potential reaches the necessary value but is retarded a certain time τ', this retardation will be the same at A_s and A_l and will therefore only affect the measurements by reducing the velocity of the discharge from A_s during the interval τ'. The measured velocity will therefore in this case be too small. It ought to be remarked, however, that we have no indications whatever of such a retardation.

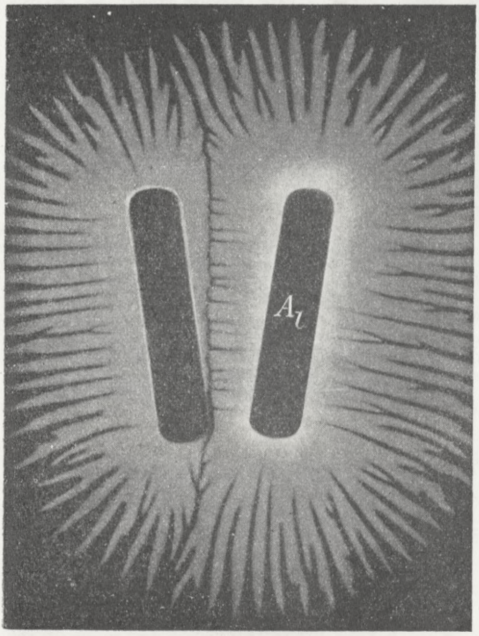

Fig. 49. Reversed Positive Velocity Figure. $L = 6$ m. (Air; $p = 75$; $l = 0.25$; $d_0 = 1.4$; $m = 0.8$).

A slowly rising wave front may influence the velocity measurements in another way. If the wire *mr* (Fig. 43) is short compared with the increasing frontal part of the wave, the increase of voltage by reflection at A_s will not attain its normal maximum value, while this will be the case at the electrode A_l, the wire *moq* being considerably longer than *mr*. The maximum voltage in this case is therefore greater at A_l than at A_s. The result hereof is that the velocity measured is too small and that the final range R_1

from A_l is greater than the range R_s from A_s (see Figs. 44, 46, and 50).

If the maximum voltage attainable by reflection from the end of the long wire *moq* is but little more than just sufficient to start the discharge, the above mentioned effect of a rather short wire *mr* may result in a — at least at first sight — rather strange phenomenon: When the wave for the first time reaches A_s the voltage does not attain such a value that a discharge takes place from A_s. At A_l, on the other hand, the voltage becomes sufficiently high and a discharge starts from this electrode. The wave reflected from A_l then travels back along *qom* and in the mean time the spark at *g* is extinguished. The wire msk_2 is in reality rather short, and the increase of voltage by reflection at A_l is now sufficient to start a discharge from A_s. The result hereof is a velocity figure exactly similar to the ordinary ones, with the sole exception that the rôles of A_s and A_l have changed. An example of such a velocity figure is shown in Fig. 49. In accordance with the explanation given the insertion of a longer wire between *m* and A_s does away with this irregularity.

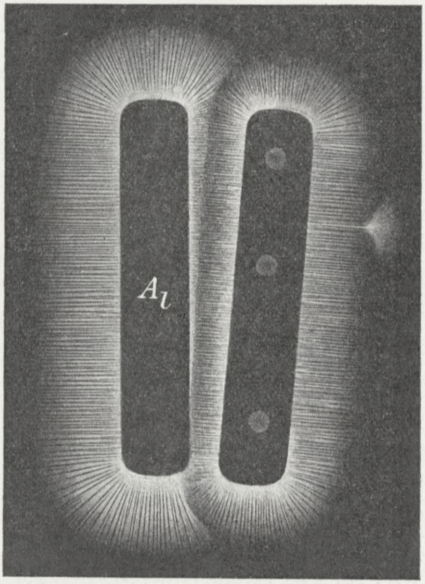

Fig. 50. Negative Velocity Figure used in the Measurement of Spark Retardation, compare Ch. VII, Fig. 72. (A_l on left Electrode should be A_2; $l_1 = 6$; $l_2 = 0.2$; no Ionization of g_2).

2. Results of the Velocity Measurements. A great

number of velocity measurements have been carried out in order to ascertain the effect of spark length, gas pressure, thickness of plate, and nature of the gas on the velocity.

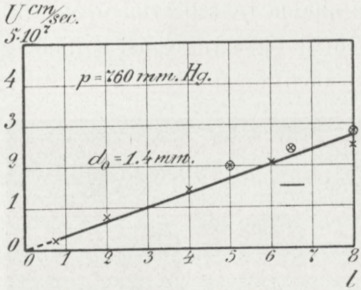

Fig. 51. Relation between Velocity U and Spark Length l for Negative Figures. (Air; $p = 760$; $d_0 = 1.4$).

Velocity of negative discharge. At atmospheric pressure the velocity U is nearly proportional to the spark length l (see Fig. 51) and the (l, U)-curve seems to pass through the origin. With a 3 mm. spark the velocity is about 1×10^7 cm/sec. At lower pressure the (l, U)-curve still starts from the origin but it is bent with the concavity against the l-axis (see the lower curves in Figs. 52 and 57).

The effect of pressure on the velocity is seen from Fig. 53. The velocity increases rapidly with decreasing pressure. As shown in the figure the experimental values fit in between the curves $U \cdot \sqrt{p} = \text{constant}$ and $U \cdot p = \text{constant}$. The last mentioned seems to give the best approximation.

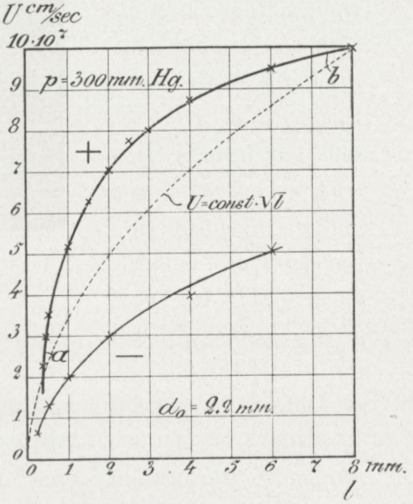

Fig. 52. Effect of Spark Length on the Positive and Negative Velocity (Air; $p = 300$; $d_0 = 2.2$).

The relation between velocity and thickness of the plate is at atmospheric pressure shown in Fig. 54. For lower pressure the velocity does not decrease so rapidly with increasing

value of d_0. In all cases the velocity seems to be greatest for very small values of d_0.

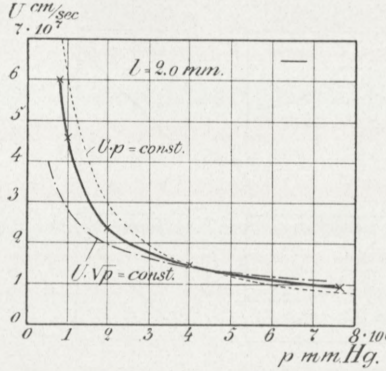

Fig. 53. Effect of Pressure on the Negative Velocity. (Air; $l=2$; $d_0=1.4$).

We may summarize the main results as follows:

1. The (l,U)-curves start from the origin.
2. The (p,U)-curves are approximately hyperbolae giving very great values for the velocity at small pressures.
3. The velocity is greatest with very thin plates.

There is a very close analogy between the dependency of the velocity upon the constants l, p, and d_0 and the dependency of the range upon the same constants. In order to illustrate this anology we have in Fig. 55 shown two sets of curves, the upper one giving the relations between range and p, d_0, and l, the lower one the corresponding curves for the velocity.

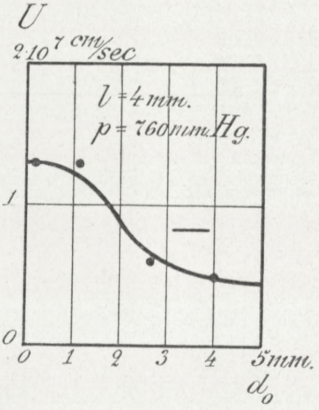

Fig. 54. Effect of Thickness of Plate on the Negative Velocity. (Air; $p = 760$; $l = 4$).

The negative velocity is very nearly the same in nitrogen and in air. For other gases measurements have not yet been made.

Velocity of the positive discharge. In air at atmospheric pressure and for spark lengths between 1.5 and 8 mm. the velocity is nearly proportional to the square root of the spark length, (see Fig. 56). At small spark lengths the velocity is, however, much smaller than according to this rule and the

velocity seems to be zero for a spark length of about .5 mm. This agrees well with the fact that no positive figure is formed

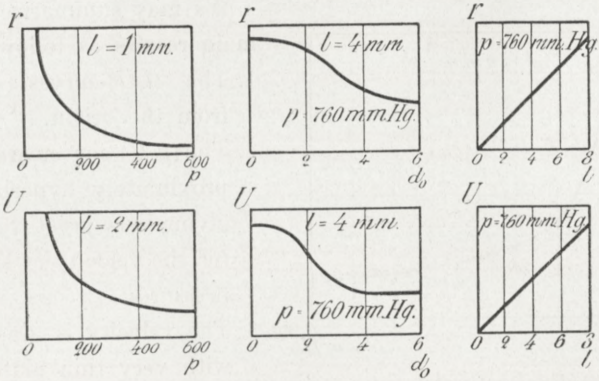

Fig. 55. Comparison between Range r and Velocity U for Negative Figures.

unless the spark length exceeds a certain value. Fig. 52 shows a (l, U)-curve corresponding to a pressure of 300 mm. hg. and Fig. 57 a similar curve for $p = 150$ mm. hg. In all three cases the general shape of the curves is the same and they all seem to start with zero velocity at some definite spark length l', where l' is roughly proportional to the pressure.

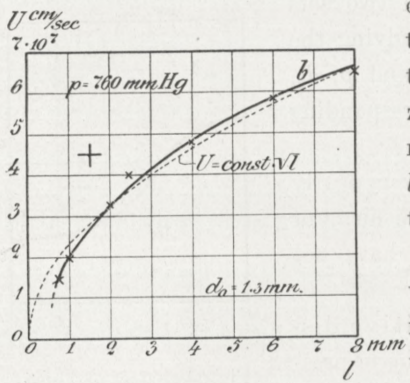

Fig. 56. Effect of Spark Length on the Positive Velocity. (Air; $p = 760$; $d_0 = 1.3$).

The relation between velocity and gas pressure is shown in Fig. 58. The velocity increases with decreasing pressure but seems to attain a definite value for very small pressures, a value which does not differ appreciably from the value for $p = 100$ mm. hg. (Fig. 58 contains only measurements

down to $p = 50$ mm. hg.; later measurements have been carried out down to $p = 20$ mm. hg. where the velocity was found to be about 5.2×10^7 cm/sec in very good agreement with the results recorded in Fig. 58).

The relation between velocity and thickness of plate is shown in Fig. 59 for a pressure of 300 mm. hg. and a spark length of 2 mm. At atmospheric pressure the (d_0, U)-curve has a similar shape; the measurements have been carried out, however, at the lower pressure, which gives a better determination of the velocity. The characteristic feature of the (d_0, U)-curve is the relatively very small values of U for small values of d_0. It seems as if U converges to zero together with d_0. The velocity curve has besides a rather marked maximum for values of d_0 about 2 to 3 mm. For great values of d_0 the velocity becomes rather small.

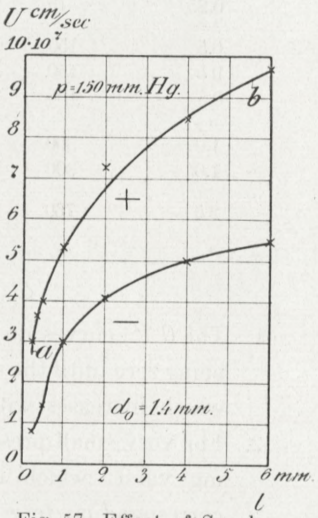

Fig. 57. Effect of Spark Length on the Positive and Negative Velocity. (Air; $p = 150$; $d_0 = 1.4$).

An examination of the different sets of measurements shows that the velocity depends upon the ratio of the pressure to the spark length, but not on these two constants separately. This relation is illustrated by the figures in Table 9, giving the results of a series of measurements in which the rate $\frac{p}{l}$ has a value of about 300. The mean value of U is 4.1×10^7 cm/sec, the highest being 4.5×10^7 and the lowest 3.8×10^7 cm/sec, that is a deviation of about ± 10 per cent from the mean value.

We may summarize the main results of our measurements of the positive velocity as follows:

Table 9. Positive Velocity in Air. p/l about 300.

Length of Spark l mm.	Air Pressure p mm. hg.	r_0 mm.	L mm.	$U = \frac{r_0}{L} . 3 \times 10^{10}$ cm/sec
0.14	40	7.6	6000	3.8×10^7
0.25	75	7.8	6000	3.9 -
0.5	150	7.8	6000	3.9 -
0.5	150	8.4	6000	4.2 -
0.5	150	24.0	16000	4.5 -
1.0	300	9.0	6000	4.5 -
1.0	300	8.4	6000	4.2 -
2.5	760	8.2	6000	4.1 -
			Mean value..	4.1×10^7

1. The (l,U)-curves do not start from the origin, the velocity being zero until the spark length has attained a certain value which increases with increasing pressure.
2. For very small pressures the velocity converges to a limiting value, which is not very different from the value corresponding to $p = 100$ mm. Hg.
3. The (d_0,U)-curves seem to start from the origin and the velocity has a maximum value for d_0 between 2 and 3 mms.
4. $U = F\left(\frac{p}{l}\right)$.

For negative figures we found a very close analogy between range and velocity in their dependency upon the constants l, p, and d_0. This analogy is, for the positive figures, violated in one important point: the (p,r)-curves and (p,U)-curves having an essentially different shape. This is the greatest difference, but the (d_0,r)-curves and the (d_0,U)-curves also show marked differences (see Fig. 60).

The positive velocity in different gases has not yet been

sufficiently investigated. We have in Table 10 quoted a few quite preliminary results.

Table 10. Positive Velocities in various Gases.

Spark Length mm.	Pressure mm. hg.	Gas	U cm/sec.
4.0	760	Air	4.8×10^7
—	—	H_2	4.5 -
0.5	150	Air	4.2 -
—	—	N_2	3.0 -
—	—	H_2	3.9 -

3. Preliminary Discussion of the Results.

The negative velocity. We have seen that the negative figures spread out from the electrode and it is therefore prob-

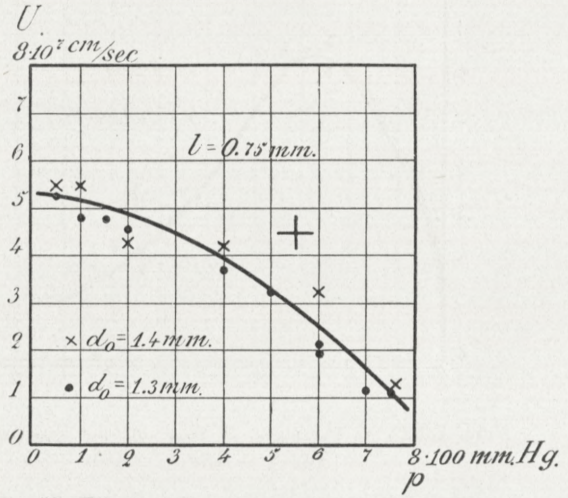

Fig. 58. Effect of Pressure on the Positive Velocity. (Air; $l = 0.75$)

able that these figures are due to electrons moving from the electrode outward under the influence of the electric field

each causing ionization by collision along its path. For the velocity of an electron moving in air under an electric force E the velocity U is determined by*)

$$U = \sqrt{2.04 \times 10^{-2} \cdot \frac{e}{m} \cdot \frac{E}{p}}, \qquad \text{(a)}$$

where E and e are in *e. s. u.* Putting $\frac{e}{m} = 5.3 \times 10^{17}$ and measuring E in volt per centimetre, this formula becomes

$$U = 6 \times 10^6 \sqrt{\frac{E}{p}} \cdot (\text{cm/sec.}). \qquad \text{(b)}$$

By the deduction of this formula it has been assumed that the velocity of an electron in the direction of the electric

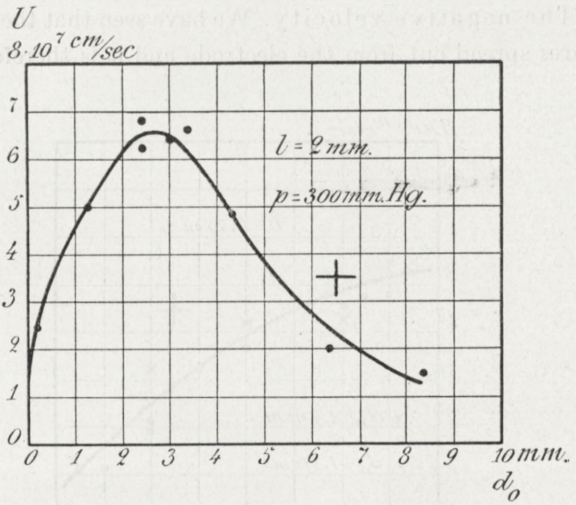

Fig. 59. Effect of Thickness of Plate on the Positive Velocity. (Air; $p = 300$; $l = 2.0$).

force greatly exceeds its velocity of agitation. These two velocities are, however, in this case approximately equal, and the above formula therefore gives too great values of U. We may write

* J. S. Townsend: Electricity in Gases. p. 343. (Oxford 1915).

$$U = \mu \cdot 6 \times 10^6 \sqrt{\frac{E}{p}}, \qquad (c)$$

where μ is a coefficient which is less than unity.

If we put $p = 760$ and $U = 2 \times 10^7$ cm/sec., corresponding to a spark length of about 6 mm. (see Fig. 51), the electric

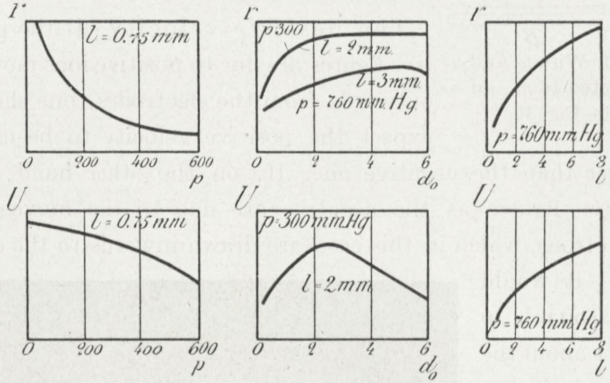

Fig. 60. Comparison of Range r and Velocity U for Positive Figures.

force is, according to formula (c), $E = \frac{1}{\mu^2}$ 8450 volts per centimetre.

This value is, no doubt, of the right order of magnitude. According to formula (c) the velocity should be proportional to the square root of the electric force and inversely proportional to the square root of the pressure. At lower pressure the velocity is nearly proportional to the square root of the spark length (see Figs. 52 and 57) while at atmospheric pressure there seems to be a straight line relation between U and l (see Fig. 51). With varying pressure the values of U fall between the values determined by $U \cdot \sqrt{p} =$ constant and by $U \cdot p =$ constant (see Fig. 53).

In view of the complicated nature of the phenomenon and in consideration of the fact that the coefficient μ depends on the ratio $\frac{E}{p}$ the above facts must be said to agree fairly well

with the supposition that the negative figures are due to electrons moving from the electrode outwards. A closer investigation of this question can, however, not be taken up with advantage before a detailed theory of the origination of these figures has been established.

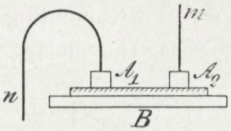

Fig. 61. Wire m and n connected to m and n in Fig. 10.

The positive velocity. If the positive figures are due to positive ions moving outwards from the electrodes, one should expect the positive velocity to be much smaller than the negative one. If, on the other hand, the positive figures as the negative are due to the movement of electrons, which in this case are drawn inwards to the electrode, it would be reasonable to expect about the same velocity for positive and negative figures and especially that the general character of the relations between the velocity and the constants l, p, and d_0 would be the same in both cases. Neither of these assumptions agree with the experimental results referred to in section 2. The positive velocity is in general found to be about 2 to 3 times greater than the negative, and the dependence of the velocities upon l, p, and d_0 shows principal differences for positive and negative figures.

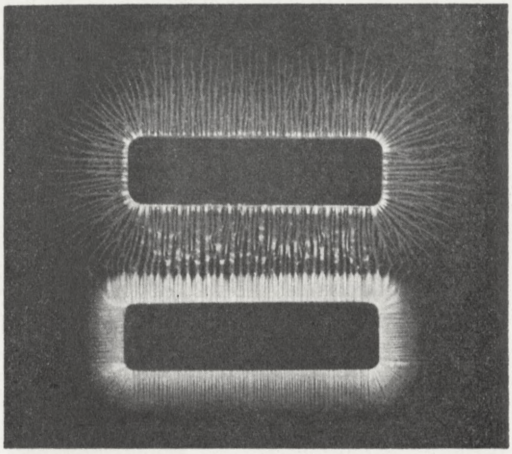
Fig. 62. Positive-Negative Figure.
(Air; $p = 760$; $l = 5$; $d_0 = 1.4$; $m = 1$).

We shall not here take up the discussion of the origination of the positive figure, we have only stated the above mentioned difficulties in order to point out the desirability of some control of our velocity measurements. One way of doing this is as follows: Two equal electrodes A_1 and A_2 were placed on the film of the photographic plate (see Fig. 61), A_1 connected to the wire n (see Fig. 10) and A_2 to m, while the electrode B was insulated by being placed on an ebonite stand. The two small and equal capacities A_2-plate-B and B-plate-A_1 are thus in series in the discharge circuit and will at the moment the discharge starts be subjected to the same voltage. For positive discharges the figure at A_2 will be positive and the A_1-figure negative, and for negative discharges the polarity of the figures will be reversed, but apart from this change in polarity the two pairs of figures are identical.

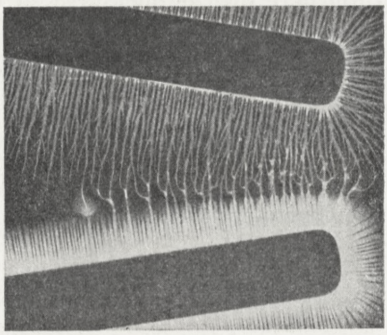

Fig. 63. Part of Positive-Negative Figure. (Air; $p = 760$; $l = 9$; $d_0 = 1.4$; $m = 0.8$).

Fig. 62 shows such a pair of figures, the two electrodes being parallel to each other. In the space between the electrodes neither the positive nor the negative figure has attained its final extension, the two figures having met each other before they were completed. In the space, where they meet, the two figures are connected by a third kind of discharge which we shall call the neutral discharge. This neutral discharge consists of a number of lines or bands of different broadness and with a soft or foggy appearance. They all form extensions of the positive trunks but differ from these by having no branches and by their foggy appearance. (These differences

are very clearly seen on the original photographs but have partly been lost in the reproduction. These neutral discharges show some other peculiarities, but we must defer the description hereof to a later occassion). Supposing the two figures start simultaneously the ratio of the distances from the electrodes to the neutral discharge will be equal to the ratio of their velocities. It will generally be more convenient to place the two electrodes at a small angle with each other, the velocity-ratio may then be measured at different points (see Fig. 63). There may be some uncertainty in measuring these distances and this method therefore only gives an approximate value of the velocity-ratio. The results obtained in this way agree, however, fairly well with those obtained with the former method as will be seen from the following table containing some of our measurements.

Table 11. Ratio of Positive and Negative Velocities Determined by Means of Simultaneous Figures.

Spark Length mm.	Pressure mm. hg.	$r_{pos.}$ mm.	$r_{neg.}$ mm.	$\frac{U_{pos.}}{U_{neg.}}$	Remarks
9.0	760	15.0	6.4	2.35	$d_0 = 2.8$ mm.
9.0	—	14.0	8.0	1.75	$d_0 = 1.3$ -
7.0	—	14.4	6.6	2.18	
5.0	—	11.0	4.5	2.45	
3.0	—	10.0	2.5	4.0	d_0 about 1.4 mm.
3.0	400	20.0	5.6	3.6	
2.0	—	18.0	3.7	4.9	
2.0	300	17.5	5.3	3.3	

Another question of some importance is whether the velocity along the surface of the plate is greater than the velocity of a sudden discharge in free air. In order to test this point we have made the following experiments: One of the electrodes in Fig. 12 was removed to a distance of 1 to 2 mm. from the plate, the other electrodes resting directly thereon.

The boundary lines between the figure around the elevated electrode and the figures from the other electrodes were thereby displaced somewhat toward the elevated electrode, but not appreciably more than what was to be expected on account of the greater distance. Even if this method does not allow anything like an exact comparison between the velocity in free air and along a plate, the experiment nevertheless indicates that there is no very great difference between the two velocities.

Chapter V.

Preliminary Theory of the Lichtenberg Figures.

1. Theory of the Negative Figures. In Chapter IV. 3. we supposed the negative figures to be due to ionization by collision produced by electrons moving outwards from the electrode. We shall now develop this working theory a little more and try to explain some of the characteristic features of the negative figures by means of it.

The very steep rise in potential caused by the electric impulse arriving at and being reflected from the electrode produces such a strong electric field in the neighbourhood of the electrode that ionization by collision sets in. This initial ionization will generally go on along the whole circumference of the electrode but with greater intensity at some points than at others. From those favourite points the negative discharge, carried by the swiftly moving electrons, will spread rapidly over the adjoining parts of the plate and thereby automatically reduce the electric force in the adjacent points at the edge of the electrode to such an extent that ionization by collision ceases to take place at these points. In this manner we get the negative discharge broken up in a number of separate flows starting from points at the edge of the electrode and distributed more or less at random along it. This question

is best illustrated by photographs taken at rather low pressure (see Fig. 28) where the distances between the starting points are greater than at higher pressure.

At some distance from the electrode the different flows have spread to such an extent that they cover the whole circumference with the exception of the thin black parting lines which we shall consider a little later. The exterior boundary of the figure will then be a circle — we suppose the electrode to be circular — the radius of which increases until the figure has attained its final size. We will now, for the sake of simplicity, suppose that the ionization is so intense in the already formed part of the figure that the drop of potential from the electrode to the front part of the figure may be neglected. In this case the density of the electric charge will be the same over the entire covered area and equal to

$$-q' = V \cdot \frac{\varepsilon}{4\pi d_0}, \qquad \text{(a)}$$

where V is the P. D. between the electrodes A and B, ε the dielectric constant of the plate and d_0 the thickness of same in centimetres. A corresponding surface density equal to $+q'$, is found on the electrode B. The free charge on the two surfaces will, however, only have a density of $-q$ and $+q$, where

$$q = \frac{V}{4\pi d_0}. \qquad \text{(b)}$$

The electric force at the edge of the figure depends on the free negative charge on the electrode A and on the developed part of the figure and the free positive charge on the electrode B. If A is not too great and if we only consider points in considerable distances from A, we may as a first approximation neglect the influence of the charge on A and only take account of the homogeneous circular charge distribution of intensity $-q$ on the surface of the plate and the corresponding charge distribution $+q$ on B. We may further

simplify our considerations by supposing that the thickness of the plate is very much smaller than the range of the figure. In this case the electric force at the edge of the figure will approximately be the same as if the figure was infinite with

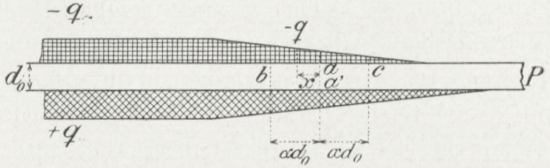

Fig. 64. Sketch of Distribution of Charge at the Edge of a Negative Figure.

a straight edge. Fig. 64 represents a cross section of such a straight edge and shows schematically the two charge distributions.

As the electric force only depends upon the free charges and as these are independent of the dielectric constant of the plate, the forces which are active in the formation of the figure and consequently also the size of the figure are independent of this constant, a result proved experimentally by W. v. Bezold.

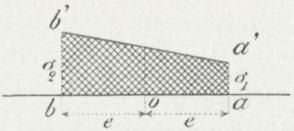

Fig. 65.

In Fig. 65 *ab* represents the cross section of a long rectilinear strip with a surface density of free electricity equal to σ_2 at b and to σ_1 at a and varying linearly from a to b. The electric force at a point o in the middle of the strip has a component in the direction oa equal to $4\,l \cdot \frac{\sigma_2 - \sigma_1}{2\,l} = -4\,l\frac{d\sigma}{dl}$, where $2\,l$ is the width of the strip and $\frac{d\sigma}{dl}$ the gradient of the charge density. We shall now consider the conditions at the edge of a figure while this figure is increasing in size due to the edge moving outwards from the electrode (see Fig. 64). The plate P rests upon the large plane metal electrode B (see Fig. 10); the horizontal component of the electric force at f. inst. the

point a' on the lower surface of P is therefore very small and may be neglected. At the point a on the upper surface of P and just opposite a' there will, however, be a considerable horizontal component, E. The effect of such parts of the charge being at a distance from aa', which is great compared with the thickness of the plate, will very nearly be the same in these two points, and the horizontal component in a must therefore mainly be due to the charges in the neighbourhood of that point, say, to the charges on the strip bc, the width of the strip being equal to $2ad_0$ where the coefficient a is considerably greater than unity, say equal to 2. If the plate is so thin that the variation in the charge can be considered as linear over the distance bc, the horizontal component will be

$$E = \mu d_0 \frac{dq}{dx}. \qquad (c)$$

where $\frac{dq}{dx}$ is the gradient of the charge density on the upper surface of P, while μ is a coefficient, which is independent of d_0. The value of q in the homogeneous part of the figure inside the edge is inversely proportional to d_0 and we may reasonably suppose the same to be the case within the edge where the density is variable. If this is so, the product $d_0 \frac{dq}{dx}$ will be independent of d_0. As the size of the figure must be determined by the intensity of the force at the edge of the figure, our theory therefore leads to the conclusion that the size with thin plates is independent of their thinness, a result which is in complete agreement with our experiments (see Fig. 33 and 34). For greater values of d_0 the distance bc in Fig. 64 becomes so great that the charge does not even approximately vary linearly between these points. The result hereof will evidently be that E diminishes. According to this theory we may therefore expect that the range decreases with increasing thickness of the plate, slowly at first with thin plates but more rapidly with thicker ones until the dist-

ance bc becomes so great as to be comparable to the range of the figures. In this case our suppositions do not apply any longer, but it is easily seen that the range will approach a certain limit when d_0 becomes very great. All these deductions agree with the experimental results.

The diffusion of the electrons along the surface of the plate must also depend on the horizontal component of the electric force. We may therefore expect that the velocity will

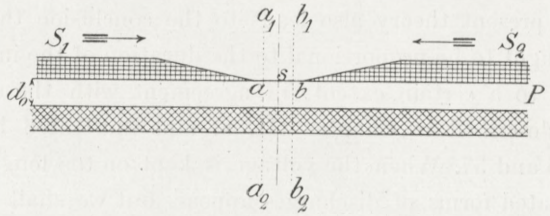

Fig. 66. Sketch of Cross Section of a Dark Line.

depend on the thickness of the plate in a similar manner as the range, a result also borne out by the experiments (see Figs. 34, 54, and 55).

We shall now consider the formation of the dark lines. The negative flow from a starting point at the edge of the electrode spreads outwards on the surface of the plate. The velocity is greatest in the radial direction but a sidewards spreading out — due to the mutual repulsion of the charge in the flow — also takes place. This lateral movement continues until the adjoining flow — moving in the opposite direction — is met. Fig. 66 is a sketch of two such flows, S_1 moving to the right and S_2 to the left. At the point s halfway between S_1 and S_2 the horizontal component E of the force is necessarily always zero, and no ionization by collision will take place there. At points to the right and left of s, E will be different from zero and varying with the time, the maximum value of E increasing with increasing distance from s. At two points

a and b, this maximum value is just sufficient to produce ionization, while between a and b no ionization will take place. The charge will diffuse over the whole surface, but no photographic impression is made between a and b, a—b thus being a cross section of a dark line. A little consideration shows that the distance between a and b, i. e. the width of the dark lines, will be very small when d_0 is very small and will increase with increasing value of d_0. This conclusion agrees with the experimental facts referred to in Chapter III.

The present theory also leads to the conclusion that the range ought to be proportional to the duration of the impulse. This is, to a certain extent, in agreement with the experiments described in Chapter III. a. and illustrated by the Figs. 36 and 37. When the voltage is kept on too long, more complicated forms of discharges appear, but we shall not at present enter into any further discussion of this point.

The present theory is certainly only a preliminary and approximative one. It does not take into account the P. D. which no doubt exists between the electrode and a point of the figure just inside the boundary region, and it does not say anything about the distribution of charge within this region. Besides, some of the approximations made are not very good. But crude as the theory is, it gives a fairly satisfactory explanation of the origination of the negative figure and of its qualities, and all the experimental facts seem to agree with our fundamental hypothesis that the negative figures are due to electrons moving outwards from the electrode and causing ionization along their path.

2. Theory of the Positive Figure. By a careful examination of all the experimental data we have collected about the positive figures, we have been led to the conclusion that these figures are due to positive particles moving outwards from the electrode. There are, however, some rather great difficulties in the way of the acceptance of this view. Some

of these difficulties have been removed while others are still outstanding. The whole question is, however, so important and its discussion will occupy so much space that it must be deferred to a later paper, where some other peculiarities of the positive discharge will also be discussed.

3. Theory of the Secondary Figure. In the sketch, Fig. 67, A and B denote as usual the electrodes, P the photographic plate with the film downwards. The line a_0ab represents diagrammatically a momentary distribution of the

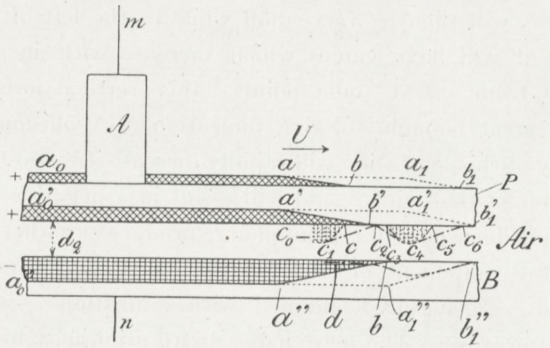

Fig. 67. Sketch of Formation of a Negative Secondary Figure.

free charge in the positive figure spreading out from A. $a_0'a'b'$ shows the corresponding induced charge at the lower surface of P, while $a_0''a''b$ represents the negative charge on the electrode B. During the formation of the primary positive figure the free charge at the upper surface of P and the induced charge on its lower surface move outwards with the velocity U of the positive discharge. If the distance between P and B is very small, so small that no considerable ionization takes place between them, the charge on B will spread in a similar manner, and no secondary figure appears. The plate P in this case, when developed, shows a more or less homogeneous blackening over the whole area below the positive figure while the intensity outside the boundary of this figure gradually

dies away. This effect on the film is due to the feeble ionization taking place in the layer of air between the plate and B.

If the distance between P and B is somewhat greater, but on the other hand not too great, say up to about 1 mm., the ionization taking place in the layer of air between P and B gives rise to certain complications, and a secondary figure generally appears. We shall now consider this process a little closer. At a certain moment the charge distribution may be as indicated in Fig. 67. The vertical component of the electric force at c_2 will then be very small while to the left of c_2 this component will have values which increase with increasing distance from c_2. At some point c this vertical force may be just great enough to give ionization by collision. The intensity of this ionization will rapidly increase if we go further to the left of the point c, and will result in a negative charge c_0c_1c being deposited on P. This charge produces a rather strong horizontal component of the electric field at c, resulting in a diffusion — generally combined with ionization — of the charge towards c_2. The new charge distribution may be represented by the line c_1c_2. In the meantime the front of the charge on the surface of P has reached the position a_1b_1, and the induced charge at the lower surface of P the position $a_1'b_1'$. The charge on the electrode B will not now be represented by the line $a_0''a_1''b_1''$ but rather by the dotted line shown between d and b_1'', and the vertical component of the electric force in the space between P and B will attain its greatest value somewhere in the neighbourhood of the point c_4. This force will cause a new ionization by collision between B and P, resulting in a negative charge $c_3c_4c_5$ being deposited on P. This charge will again diffuse especially towards c_6. And so on. For the explanation of the positive secondary figure it is only necessary to reverse the sign of all charges.

It follows from this explanation that the lines of the negative secondary figures should have the same soft and foggy

appearance which characterises the boundary of the negative figure. On the outer side of the lines of the positive secondary figures we may, on the other hand, expect to find offshoots of a positive character being due to lateral diffusion of the accumulated positive charges. The secondary lines will evi-

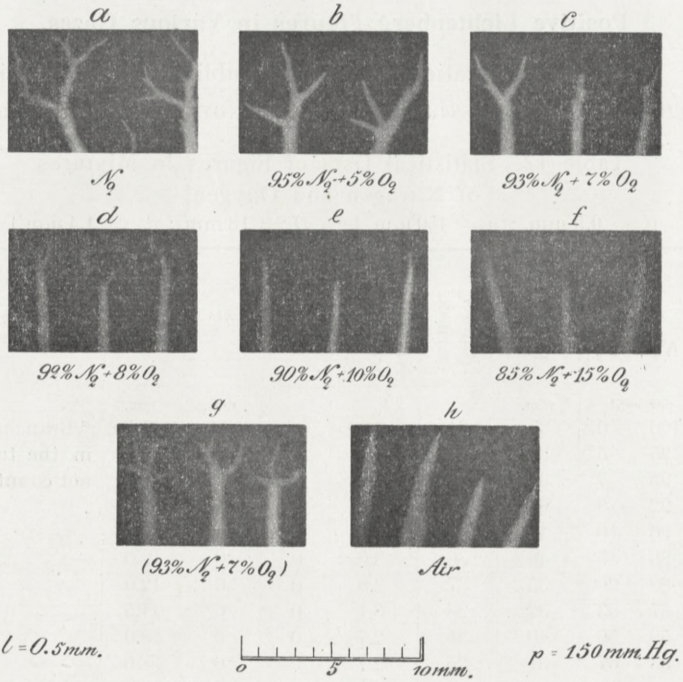

Fig. 68. Tops of Trunks of Positive Figures in Mixtures of Nitrogen and Oxygen. Part *g* in Nitrogen from Steel Flask.

dently have a tendency to be parallel with the simultaneous boundary of the primary figure, but if some obstacle is placed in the space between *P* and *B*, it is easily conceived that a secondary line will often start from the boundary of such an obstacle. It is to be expected that the distance between the secondary lines will increase with increasing distance between *P* and *B* and with decreasing charge. On all these points theory

and experiment agree completely with each other. This theory also explains why there are no secondary figures directly below the electrode A.

Chapter VI.

Positive Lichtenberg Figures in Various Gases.

Very few observations have been published about positive figures in other gases than air. E. Reitlinger (1861)[2] noted that

Table 12. Statistical Data of Figures in Mixtures of Nitrogen and Oxygen.
(l = 0.5 mm.; p = 150 mm. hg. D = 18 mm.; d_0 = 1.4 mm.).

Gas		Range r	Number of trunks	Number of branches on each trunk	a^1	b^1	c^1	Remarks
N_2	O_2							
per cent		mm.				mm.	mm.	
100	0	35	34	2.9*	4.4	13.5	9.5	* Branches
95	5	35	30	2.6	2.6	7.9	12.5	in the top
93	7	37	30	2.8	1.7	3.0	12.0	not counted
92	8	37	34	2.8	1.0	1.1	12.2	
90	10	42	32	2.9	0.9	0.5	13.0	
85	15	40	36	3.0	0	0	12.0	
80	20	35	37	2.9	0	0	12.0	
67	33	32	28	3.1	0	0	11.5	
50	50	40	35	2.7	0	0	8.0	
33	67	31	25	2.7	0	0	6.0	
Mean value . .		36.4	32.1	2.74				

[1] Column a contains the average number of branches in the top, only branches exceeding 1 mm. in length being counted. A pointed end of a trunk is counted as a branch. Column b contains the average value of the total length of all the branches per top. Column c the average length of branch-free trunk just below the top.

a figure in hydrogen has more branches than a figure in air. W. Holtz (1905)[1] is of the opinion that the nature of the gas is of very little importance. S. Mikola (1917)[1] states, that the figures in air and in nitrogen of atmospheric origin are similar and that figures in oxygen, hydrogen, carbon dioxide

and coal gas are so faint as to be almost invisible. We have taken some series of positive figures in nitrogen, oxygen, hydrogen, and different mixtures of these gases. Occasionally a figure has been taken in carbon dioxide and in a mixture of argon and air. All these experiments have been of a wholly

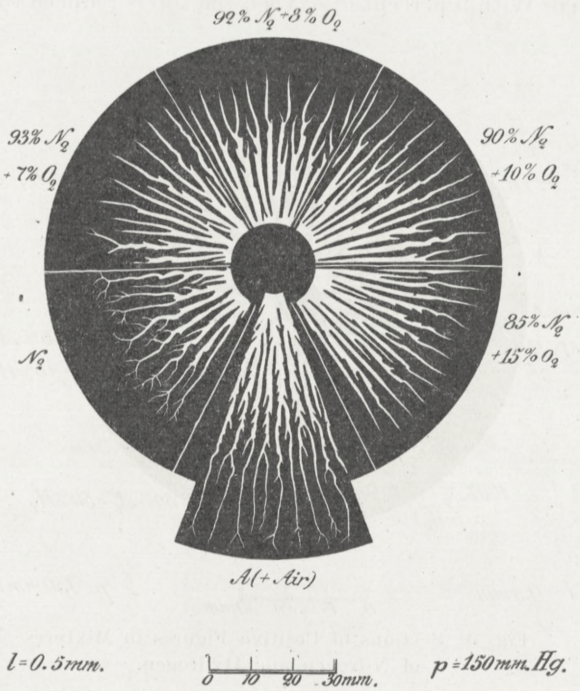

Fig. 69. Sections of Positive Figures in Mixtures of Nitrogen and Oxygen. (Lower Section in Argon + Air).

preliminary nature, but some of the obtained results may be of sufficient interest to be quoted here.

Mixture of nitrogen and oxygen. In pure nitrogen the figures are very clear and intense, the trunks and the thick branches being almost black on the developed plate, the top branches being somewhat »weaker« and not so sharply defined. With increasing percentage of oxygen the figure be-

comes fainter and with 1 per cent nitrogen and 99 per cent oxygen it is just visible.*) But other and more striking alterations take place. In pure nitrogen there is a well developed top consisting of a system of branches at the end of each trunk. With increasing percentage of oxygen this is greatly reduced. With 5 percent of oxygen the top is reduced to about

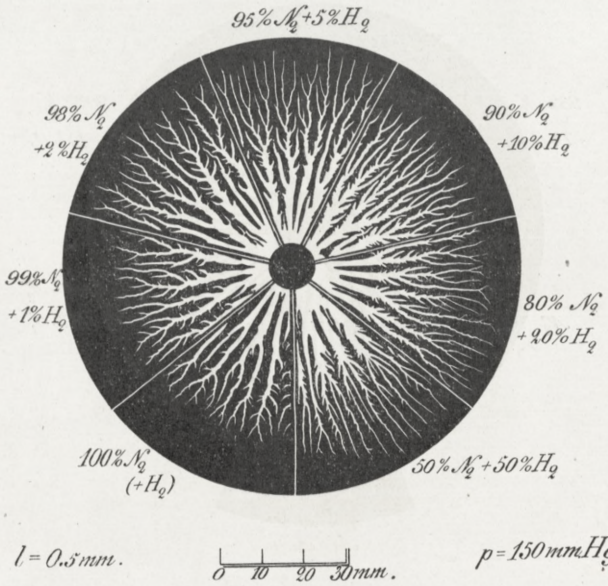

Fig. 70. Sections of Positive Figures in Mixtures of Nitrogen and Hydrogen.

half size and the remaining branches are stouter and more trunk like (see Fig. 68). With 7 per cent oxygen many of the trunks have no top at all but only some short irregular branches at the end of each trunk. With 10 per cent oxygen the trunks have a pointed end but no branches, and with still more oxygen the trunks are but ended. An increase in the percentage of oxygen beyond 15 does not seem to cause any great alteration in the shape of the figure with the exception that the

* All figures refer to per cent of volume.

outermost branchless part of the trunks becomes shorter. Neither the number of trunks nor the number of branches en each trunk — the branches in the top not being counted — seems to depend on the composition of the mixture; the whole offect of the oxygen is that it cuts away the top of the pure

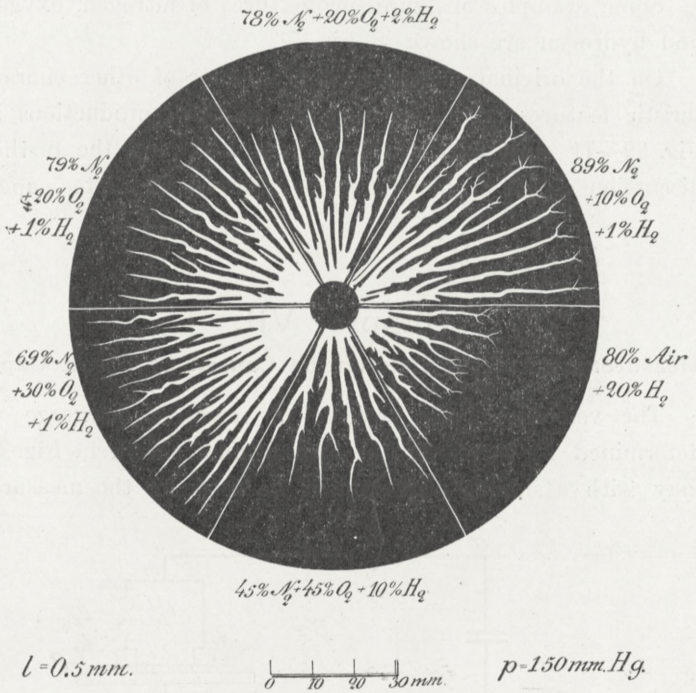

Fig. 71. Sections of Positive Figures in Mixtures of Nitrogen, Oxygen, and Hydrogen.

nitrogen figure. In order to illustrate these points further, we have in Fig. 69 shown sections of figures in different mixtures of nitrogen and oxygen (and a sector of an argon air figure), but most of the details of the tops have unfortunately been lost in the reproduction. Some statistical data about figures in such mixtures have been collected in Table 12.

Mixtures of nitrogen and hydrogen. The effect of hydrogen is mainly to create a great number of short branches on the middle parts of the trunks while the influence on the top is much less pronounced. Sections of such figures are shown in Fig. 70.

Some examples of figures in mixtures of nitrogen, oxygen and hydrogen are shown in Fig. 71.

On the original photographs a number of other characteristic features are to be seen but in the reproductions in Fig. 69—71 most of these have been lost, and the further discussion of this problem must be deferred till a later paper.

Chapter VII.

Measurements of the Retardation Caused by Spark Gaps.

The velocity of the positive or negative discharge as determined by means of the arrangemnet shown in Fig. 43 may with a similar arrangement be used for the measure-

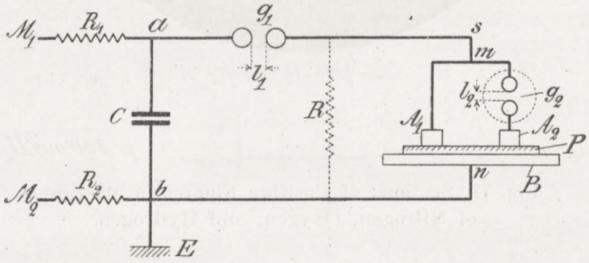

Fig. 72. Sketch of Arrangement for Measuring Spark Retardation.

ment of very short intervals of time. As an example hereof we shall quote some measurements made by this method of the retardation caused by spark gaps. A sketch of the arrangement is shown in Fig. 72. The spark gap g_2 is enclosed in a tube of insulating material, and the inside of this tube

may either be kept dark or the spark gap exposed to the light from a d. c. arc at a distance of 20 cm. from g_2. We call the two states of the gap respectively the normal and the ionized. The spark gap g_2 is inserted in a wire leading from the point m to the electrode A_2, another similar wire of equal length leading from m to the electrode A_1, equal to A_2. If there was no retardation in the gap g_2, the discharges from A_1 and A_2, caused by a spark in g_1, would start simultaneously and meet midway between A_1 and A_2. The retardation actually caused by g_2 can now be measured by determining the range r_0 of the discharge from A_1 at the moment the discharge from A_2 starts. The retardation T is then equal to

$$T = \frac{r_0}{v},$$

where v is the known velocity of the discharge from A_1.

Table 13 contains some results of a set of such measurements.

Table 13. Retardation Caused by Spark Gaps in Air at Atmospheric Pressure. Measured by Means of Negative Figures. Velocity $v = 2.5 \times 10^7$ cm/sec.)

Spark Length		Spark Gap	r_0	$T = \frac{r_0}{2.5 \times 10^7}$
l_1	l_2	g_2		
mm.	mm.		mm.	sec.
6.0	1.0	normal	> 12.5	$> 5.0 \times 10^{-8}$
—	—	ionized	5.0	2.0×10^{-8}
—	—	ionized	5.5	2.2×10^{-8}
6.0	0.2	normal	6.5	2.6×10^{-8}
—	—	ionized	2.5	1.0×10^{-8}
6.0	0.1	normal	3.0	1.2×10^{-8}
—	—	ionized	0.5	0.2×10^{-8}

We have thus been able to measure the retardation caused by an ionized spark gap whose length is only about a hundredth part of the maximum spark length. By using positive

figures at a lower pressure it is possible to measure fairly accurately intervals down to or even below 1×10^{-9} second.

The influence of different physical conditions on the retardation of sparks is most easily studied by comparing two spark gaps, one placed between m and A_1, the other between m and A_2 (see Fig. 72).

I wish to express my indebtedness to Mr. O. Ellekilde for his assistance in some of these experiments and to Mr. J. P. Christensen for his valuable help in the whole investigation.

Royal Technical College of Copenhagen,
September 1918.

Meddelt paa Mødet d. 8. Marts 1918.
Færdig fra Trykkeriet d. 12. Februar 1919

Bibliography.

K. Antolik: 1. Über neue electrische Figuren und über das Gleiten electrischer Funken. Wied. Ann. 15 p. 475—491. 1882

W. G. Armstrong: 1. Electric Movement in Air and Water. First Ed. London 1897.

— 2. Second Ed. with a Supplement by Armstrong and H. Stroud London 1899.

W. v. Bezold: 1. Untersuchungen über elektrische Staubfiguren. Pogg. Ann. 140. p. 145—159. 1870.

— 2. Untersuchung über die electrische Entladung. Pogg. Ann. 140. p. 541—552. 1870.

— 3. Über die Zerlegung einer Entladung in Partialentladungen. Pogg. Ann. 140. p. 559—560. 1870.

— 4. Über das Bildungsgesetz der Lichtenbergschen Figuren Pogg. Ann. 144. p. 337—363, 526—550. 1871.

— 5. Über Lichtenberg'sche Figuren und elektrische Ventile. Wied. Ann. 11. p. 787—795. 1880.

— 6. Über die Untersuchung elektrischer Drahtwellen mit Hülfe von Staubfiguren. Wied. Ann. 63. p. 124—131. 1897.

E. W. Blake: 1. A Method of Producing, by the Electric Spark, Figures Similar to Those of Lichtenberg. Am. Journ. of Sc. and Arts. (2). 49. p. 289—294. 1870.

J. Brown: 1. On Figures Produced by Electric Action on Photographic Dry Plates. Phil. Mag. (5) 26. p. 502—505. 1888.

K. Bürker: 1. Über ein Dreipulvergemisch zur Darstellung elektrischer Staubfiguren. Ann. d. Phys. (4). 1. p. 474—482. 1900.

M. Esch: 1. Über den Vorprocess und die Verzögerung bei der Funkenentladung. Diss. 1908. 57. pp.

K. Hansen: 1. Photographie elektrischer Entladungen. E. T. Z. 37. p. 610—611. 1916.

W. Holtz: 1. Über die Lichtenbergschen Figuren und ihre Entstehung. Phys. Z. 6. p. 319—328. 1905.

— 2. Zur Darstellung Lichtenbergscher Figuren in Vorlesungen. Phys. Z. 7. p. 162—163. 1906.

G. C. Lichtenberg: 1. Nova methodo naturam ac motum fluidi electrici investigandi. Commentatio prior. Novi Commentarti Soc. Reg. Sc. Gottingensis. T. 8. p. 168—180. 1778.
— 2. Commentatio posterior. Commentationes Soc. Reg. Sc. Gott. Classis mathematicae T. 1. p. 65—79. 1779.
R. Mach und S. Doubrava: 1. Beobachtungen über die Unterschiede der beiden electrischen Zustände. Wied. Ann. 9. p. 61—76. 1880.
S. Mikola: 1. Untersuchungen über die Lichtenbergschen Figuren und über die Strahlung des Kondensators. Phys. z. 18. p. 158—168. 1917.
G. Quincke: 1. Über elektrischer Staubfiguren auf Isolatoren und durchgehende, reflektierte, sekundäre und rückläufige elektrische Strahlen. Ann. d. Phys. (4). 32. p. 91—147, 889—940. 1910.
E. Reitlinger: 1. Zur Erklärung der Lichtenbergschen Figuren. Sitzungsber. d. Wien. Akad. Math.-nat. Cl. 41. p. 358—376. 1860.
— 2. Vorläufige Note über Lichtenberg'sche Figuren in verschiedenen Gasen. Sitzungsber. d. Wien. Akad. Math.-nat. Cl. 43. p. 25—26. 1861.
P. T. Riess: 1. Über elektrische Figuren und Bilder. Abh. d. K. Akad. d. Wiss. Berlin. p. 1—50. 1846.
— 2. Reibungselektricität. Bd. 1—2. Berlin 1853.
S. P. Thompson: 1. On the Cause of the Difference in Lichtenberg's Dust-Figures. Preliminary Note. Proc. Roy. Soc. London. 58. p. 214—215. 1895.
M. Toepler: 1. Über den inneren Aufbau von Gleitbüscheln und die Gesetze ihrer Leuchtfäden. Ann. d. Phys. (4). 53. p. 217—234. 1917.
E. T. Trouvelot: 1. Sur la forme des décharges électriques sur les plaques photographiques. La lumiére élec. 30. p. 269—273. 1888.
A. v. Waltenhofen: 1. Über den Lullin'schen Versuch und die Lichtenberg'schen Figuren. Pogg. Ann. 128. p. 589—609. 1866.
K. Wesendonck: 1. Untersuchungen über Büschelentladungen. Wied. Ann. 30. p. 1—50. 1887.
G. Wiedemann: 1. Über das elektrische Verhalten krystallisirter Körper. Pogg. Ann. 76. p. 404—412. 1849.

Contents.